European Journal of Medicinal Chemistry 249 (2023) 115163

Contents lists available at ScienceDirect

European Journal of Medicinal Chemistry

journal homepage: www.elsevier.com/locate/ejmech

Research paper

Novel S1R agonists counteracting NMDA excitotoxicity and oxidative stress: A step forward in the discovery of neuroprotective agents

Pasquale Linciano [a], Claudia Sorbi [b], Giacomo Rossino [a], Daniela Rossi [a], Andrea Marsala [c], Nunzio Denora [d], Martina Bedeschi [e], Noemi Marino [e], Giacomo Miserocchi [e], Giulio Dondio [f], Marco Peviani [c], Anna Tesei [e], Simona Collina [a], Silvia Franchini [b,*]

[a] Department of Drug Sciences, University of Pavia, Viale Taramelli 12, 27100, Pavia, Italy
[b] Department of Life Sciences, University of Modena and Reggio Emilia, 41125, Modena, Italy
[c] Department of Biology and Biotechnology "L. Spallanzani", University of Pavia, 27100, Pavia, Italy
[d] Dipartimento di Farmacia – Scienze del Farmaco, Università, degli Studi di Bari Aldo Moro, 70126, Bari, Italy
[e] BioScience Laboratory, IRCCS Istituto Romagnolo per lo Studio dei Tumori (IRST) "Dino Amadori", 47014, Meldola, Italy
[f] Aphad SrL, Via della Resistenza, 65, Buccinasco, 20090, Italy

A B S T R A C T

Sigma-1 receptor (S1R) has been considered a promising therapeutic target for several neurodegenerative diseases and S1R agonists have shown neuroprotective activity against glutamate excitotoxicity and oxidative stress. Starting from a previously identified low nanomolar S1R agonist, in this work we prepared and tested novel benzylpiperidine/benzylpiperazine-based compounds designed by applying a ring opening strategy. Among them, 4-benzyl-1-(2-phenoxyethyl)piperidine **6b** (S1R *Ki* = 0.93 nM) and 4-benzyl-1-(3-phenoxypropyl)piperidine **8b** (S1R *Ki* = 1.1 nM) emerged as high affinity S1R ligands and showed selectivity over S2R and N-methyl-D-aspartate receptor (NMDAR). Candidate compounds behaved as potent S1R agonists being able to enhance the neurite outgrowth induced by nerve growth factor (NGF) in PC12 cell lines. In SH-SY5Y neuroblastoma cell lines they exhibited a neuroprotective effect against rotenone- and NMDA-mediated toxic insults. The neuroprotective activity of **6b** and **8b** was reverted by co-treatment with an S1R antagonist, PB212. Compounds **6b** and **8b** were tested for cytotoxicity *in-vitro* against three human cancer cell lines (A549, LoVo and Panc-1) and *in-vivo* zebrafish model, resulting in a good efficacy/safety profile, comparable or superior to the reference drug memantine. Overall, these results encourage further preclinical investigations of **6b** and **8b** on *in-vivo* models of neurodegenerative diseases.

1. Introduction

Chronic neurodegenerative diseases, such as Alzheimer's disease (AD), Parkinson's disease (PD), Huntington's disease, amyotrophic lateral sclerosis (ALS) and multiple sclerosis (MS) still represent a great challenge for pharmacological research, since available treatments are mainly symptomatic and present side effects and limitations [1–3]. The World Health Organization (WHO) estimates the cost of neurodegenerative disorders in the European Union (EU) alone to be more than 160 Billion Euro per year [4]. This cost will continue to rise dramatically due to Europe's demographic aging [5]. The development of new drugs for a disease-modifying therapy, able to halt or to reverse the progression of these pathologies, would represent a paradigm shift in the treatment of the neurodegenerative disorder [6,7]. This requires the necessity to identify or exploit novel molecular targets. Sigma 1 receptor (S1R) has gained particular attention among the potential therapeutic targets [8–10]. S1R is highly expressed in neurons and glia of multiple regions within the central nervous system (CNS) where it is involved in neuroprotection, neuroinflammation, neurotransmission, and neuroplasticity. Indeed, S1R is implicated in several neurodegenerative disorders (such as memory and cognition disorders including AD, HD, and ALS). Deficits or dysfunction in S1R are associated with neurodegeneration. Conversely, activating S1R can convey neuroprotective effects by rescuing cells from damage, promoting neuronal survival, and restoring neuronal plasticity which in turn can slow the progression of the disease. The S1R is also involved in cancer cell physiology and overexpressed in a variety of tumours, suggesting its protective role in cancer cell survival and tumour progression [11–13]. At cellular level, S1R is a chaperone-like protein primarily localized at the mitochondria-associated endoplasmic reticulum membranes or MAMs. Upon activation, S1R de-oligomerizes [14] and interacts with receptors and ion channels which leads to changes in calcium balance, integrity of endoplasmic reticulum (ER) and mitochondria, and reduction of oxidative and nitrosative stress (Fig. 1). One of the most studied

* Corresponding author.
E-mail address: silvia.franchini@unimore.it (S. Franchini).

https://doi.org/10.1016/j.ejmech.2023.115163
Received 9 November 2022; Received in revised form 24 January 2023; Accepted 25 January 2023
Available online 26 January 2023
0223-5234/© 2023 The Authors. Published by Elsevier Masson SAS. This is an open access article under the CC BY license (http://creativecommons.org/licenses/by/4.0/).

neuroprotective effects mediated by S1R is the functional balance of the NMDAR activity. Indeed, on the one hand, S1R enhances the function of NMDAR, thus eliciting signalling cascades that strengthen the communication between synapses contributing to synaptic plasticity and improving learning and memory. However, since an excessive influx of calcium via overactivated NMDAR can cause excitotoxicity, on the other hand, S1R counteracts Ca^{2+} dyshomoeostasis by promoting the entry of Ca^{2+} into the mitochondria. Furthermore, S1R contributes to the reduction of NMDAR-mediated NO production and nitrosative stress overall [15–17]. In addition to NMDAR mediated effects, S1R may also contribute to neuroprotection through the mitigation of ROS accumulation, possibly through the modulation of ROS-neutralizing proteins [18]. Moreover, S1R may exert a potential role as a gatekeeper for endoplasmic reticulum (ER) stress [19,20], triggering the terminal unfolded protein response (UPR) [20], a condition that numerous studies have closely correlated with aging-associated diseases, including cancer [21–24]. Lastly, S1R is also found in microglia, where it regulates the activity of microglia and reduces neuroinflammation by suppressing the production of proinflammatory cytokines and chemokines [25].

Several studies have shown the potential benefits of using S1R agonists in treating or reversing the progression of AD, PD, MS, and SLA [26–38]. To date, three S1R agonists are in clinical trials for the treatment of neurodegenerative disease named blarcamesine, cutamesine and pridopidine (Fig. 2). Blarcamesine (or ANAVEX 2–73), a mixed muscarinic receptor/S1R ligand [39], is currently being tested in phase III clinical trials for AD [40] and phase II clinical trials for cognitive impairment in PD patients with dementia [41] and Rett syndrome [42, 43]. Cutamesine has completed a phase II clinical trial for the treatment of acute ischemic stroke and major depression [44]. Lastly, pridopidine is currently being evaluated in a phase II clinical trial for treating levodopa-induced dyskinesia in patients with Parkinson's disease [45]. It has previously completed a phase III clinical trial, where it showed promising results in treating motor symptoms in Huntington's disease [46,47]. These success stories encourage the seeking for S1R agonists and deliver additional guidance for new S1R drug candidates that might represent the next generation of psychotherapeutic agents.

For many years, our research group has been active in the field of sigma receptor modulators and low nanomolar and sub-nanomolar ligands, designed by combining different substituted five-member heterocyclic rings with appropriate pharmacophoric amines (i.e., benzylpiperidine and benzylpiperazine), have been identified (Fig. 3) [48–51]. In particular, compounds **I–V** displayed neuroprotective abilities, rescuing neuronal cells from oxidative stress and NMDA-induced toxicity. Compound **II,** a full S1R agonist, was the most selective with 70-fold selectivity for S1R over S2R.

In the present work, starting from compound **II**, we applied a ring opening strategy to explore the effect of the oxathiazole ring on S1R binding affinity and selectivity (Fig. 4). A new series of acyclic derivatives was prepared. The compounds were tested in a cell-based assay for agonist/antagonist behaviour and the best compounds were subjected to efficacy studies to evaluate their neuroprotective capability. In addition, early toxicity studies were performed to assess the drugability profile for further preclinical investigation on animal models of neurodegenerative diseases.

2. Results and discussion

2.1. Compound design

Sixteen new acyclic derivatives were designed by replacing the 1-oxa-4-thiaspiro[4.5]decan portion of **II** with bioisosteric alkylene linkers (**1a-8a** and **1b-8b**, Table 1).

All the accessible combinations deriving from the linearization of the 1-oxa-4-thiaspiro[4.5]decan ring were considered. The heterocyclic linker of **II** was therefore converted in an ethylic or propylic aliphatic chain and connected to the primary hydrophobic moiety by means of an ether or a sulphide linker. Recent studies revealed the requirement of an alkylene linker with an H-bond acceptor substituent, such as S or O, between the amine and the primary hydrophobic portion of a S1R ligand, as an important feature for S1R binding [52]. Moreover, the importance of a saturated or aromatic carbocycle, as primary hydrophobic moiety, was investigated by replacing the cyclohexyl ring of the lead compound with the phenyl ring. As far as concern the ionizable amine, based on our previous SAR investigation both benzyl-piperazine or benzyl-piperidine derivatives were considered in the design of the new linearized derivatives. Because these molecules have to reach the CNS, the most relevant physicochemical and drug-likeness properties of the designed set of compounds were profiled in silico using the SwissADME web utility [53]. According to the international guideline, particular attention was posed on those attributes accounting for a

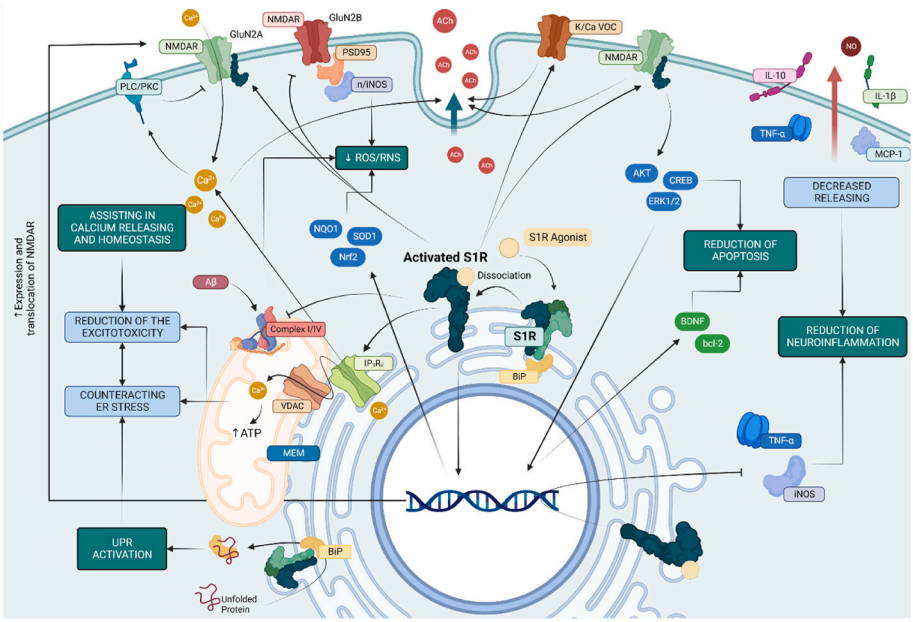

Fig. 1. Main physiological pathways elicited by S1R activation and implicated in neuroprotection (Created with BioRender.com).

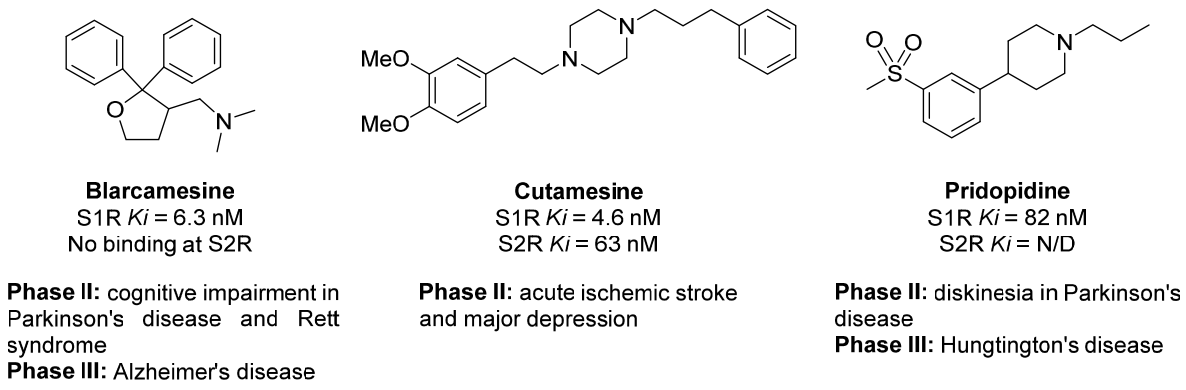

Fig. 2. S1R agonists currently in clinical trials: chemical structures, binding affinity at S1R and S2R and therapeutic indications.

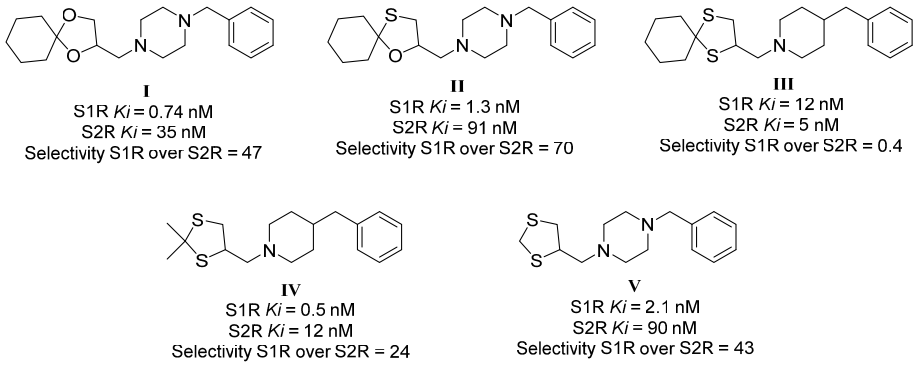

Fig. 3. Chemical structures and SRs binding affinity and selectivity of the most promising compounds of our library of SR modulators endowed with neuroprotective efficacy.

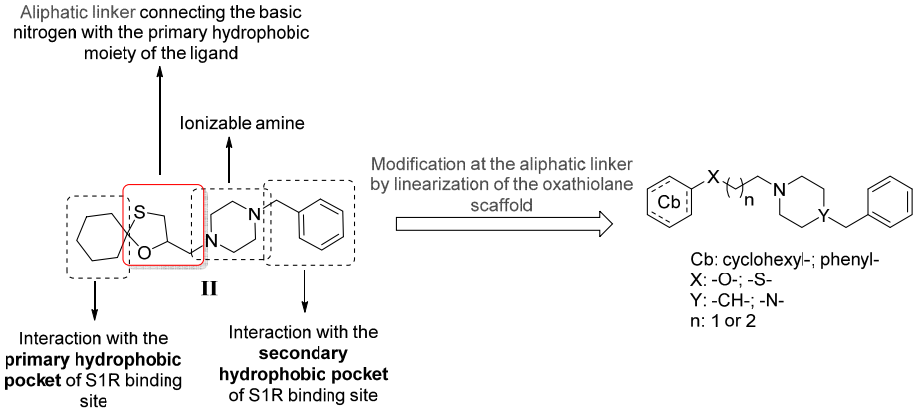

Fig. 4. Rational design of the new linear derivatives of compound **II**.

successful CNS drug [54,55]. The predicted physicochemical properties for the 16 designed compounds are resumed in **Tables SI–1** and are represented in an intuitive graphical classification model viz. BOILED-Egg diagram as shown in Fig. 5. All the designed compounds are predicted to be absorbed *per os* and to be able to cross the BBB, indicating an overall balanced physicochemical profile for optimal brain exposure. Lastly, all the compounds passed the check for pan-assay interference compounds (PAINS) evaluated with the in-silico tool FAF-Drugs4 [56].

Table 1
Chemical structures of the new designed compounds **1a-8a** and **1b-8b**.

	Piperazine derivates	Piperidine derivates
Cyclohexyl Derivates	**1a** 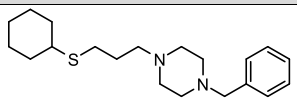	**1b** 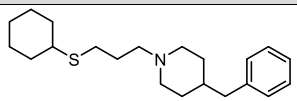
	2a 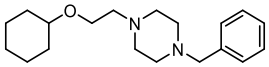	**2b** 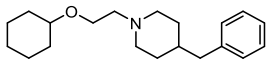
	3a 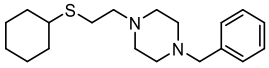	**3b** 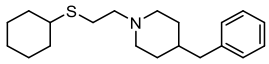
	4a 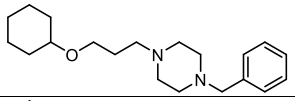	**4b** 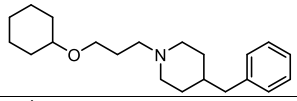
Phenyl Derivates	**5a** 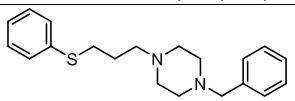	**5b** 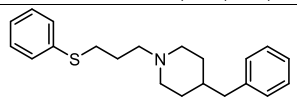
	6a 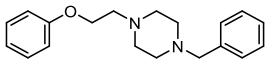	**6b** 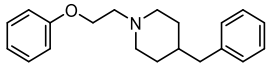
	7a 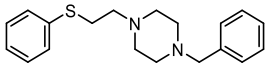	**7b** 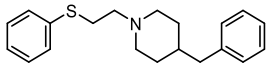
	8a 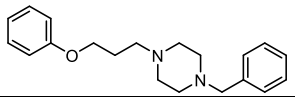	**8b** 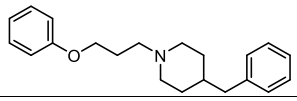

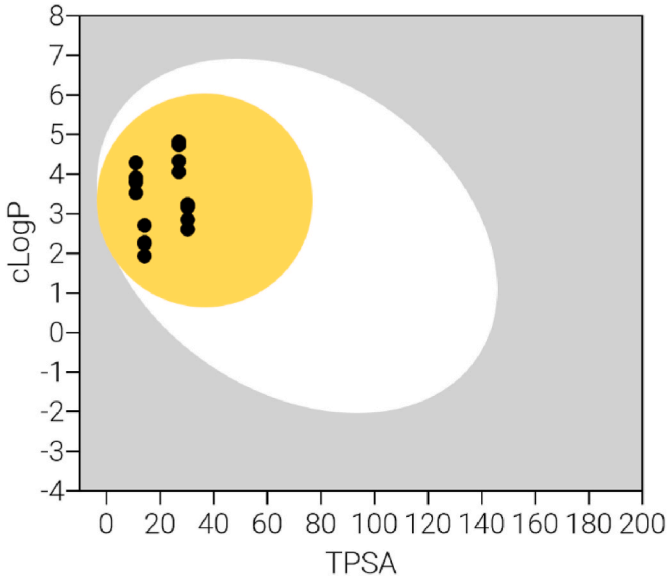

Fig. 5. Boiled-egg diagram for the designed compounds (**1a-8a** and **1b-8b**). The white region defines the physicochemical space of molecules with highest probability of being absorbed by the gastrointestinal tract, and the yellow region (egg yolk) defines the physicochemical space of molecules with highest probability to permeate to the brain.

2.2. Chemistry

The synthesis of amines **1a-b** is reported in Scheme 1. Cyclohexanethiol was reacted first with 1,3-dibromopropane in standard S_N2 conditions, in acetone at room temperature for 24 h, using K_2CO_3 as base, to give the thioether **9** in a 50% yield (Scheme 1). 1,3-Dibromopropane was used in large excess (3 equivalents with respect to cyclohexanethiol), in order to avoid the formation of the disubstituted product. However, despite the complete consumption of the starting thiol, the modest yield achieved for **9** could be imputed to the unavoidable formation of the cyclohexyldisulphide (due to the easily oxidation of thiols in alkaline environment) and to the cumbersome chromatographic purification required to isolate the product of interest from the excess of unreacted dibromopropane. The S_N2 reaction of **9** with 4-benzylpiperidine or 1-benzylpiperazine, in DMSO, at room temperature, in the presence of K_2CO_3 to neutralize the forming hydrobromic acid, afforded compounds **1a** and **1b** in a 60% and 80% yield, respectively (Scheme 1).

For the synthesis of the cyclohexyl ethylenic ethers **2a-b**, the commercially available 2-(cyclohexyloxy)ethan-1-ol (**10**) was converted into the corresponding aliphatic chloride (**11**) by reaction with refluxing thionyl chloride, in the presence of a catalytic amount of DMF. Finally, **11** was reacted with 4-benzylpiperidine or 1-benzylpiperazine as described above to give compounds **1a** and **2b** with a 25% and 45% of yields, respectively (Scheme 2).

Conversely, the synthesis of the sulphurated bioisosters of **2a-b** (namely, **3a-b**) followed a different synthetic approach (Scheme 3). Cyclohexanethiol and ethyl bromoacetate were reacted in acetone at room temperature for 6 h in the presence of K_2CO_3 to give ethyl 2-(cyclohexylsulfanyl)acetate (**12**) in quantitative yield [57]. The intermediate **12** was then hydrolysed to the corresponding carboxylic acid (**13**) using mild conditions such as 1 N aqueous NaOH in THF/EtOH 3:1 at room temperature for 6 h. The carboxylic acid **13** was further reacted with 1-benzylpiperazine (for **14a**) or 4-benzylpiperidine (for **14b**) in the presence of EDC and HOBt as coupling agents, in DMF, at 0 °C for 1 h and then at room temperature overnight, to give the corresponding amides **14a-b** (Scheme 4). Finally, amides **14a-b** were reduced to the corresponding amines **3a-b** with $LiAlH_4$ in dry THF under argon atmosphere at 0 °C for 1 h and then at room temperature overnight (Scheme 4).

The synthesis of the final compounds **4a-b** required the preparation of the cyclohexyl propyl ether intermediate **16,** first. Accordingly, cyclohexanone was condensed with 1,3-propandiol in refluxing toluene,

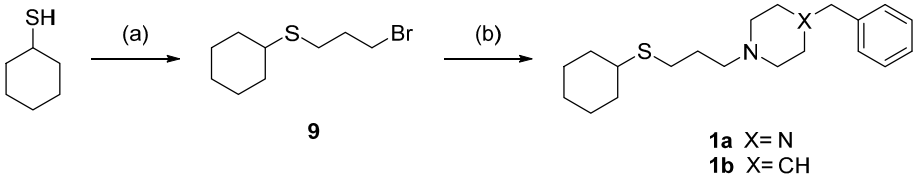

Scheme 1. Reagents and conditions: a) 1,3-Dibromopropane (3 eq.) and K_2CO_3 (2.5 eq.), acetone, r.t., 24 h, 50% yield. b) 4-benzylpiperine or 1-benzylpiperazine (1.2 eq.), K_2CO_3 (2.5 eq.), DMSO, r.t., 3 h–18 h, 62% yield (for 1a) and 81% yield (for 1b).

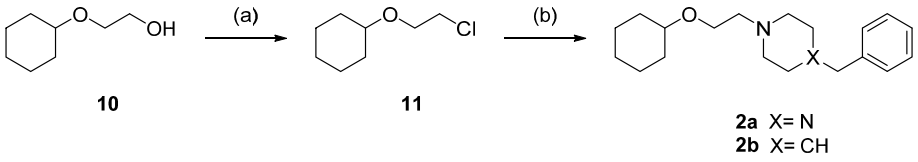

Scheme 2. Reagents and conditions: a) $SOCl_2$, neat, reflux, 2 h, 57% b) 4-benzylpiperine or 1-benzylpiperazine (1.2 eq.), K_2CO_3 (2.5 eq.), DMSO, r.t., 24 h, 20% yield (for 2a) and 45% yield (for 2b).

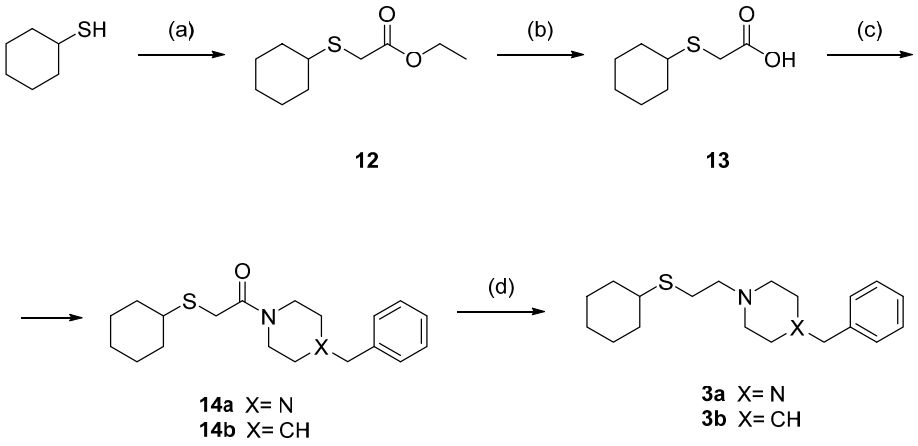

Scheme 3. Reagents and conditions: a) K_2CO_3 (2.5 eq.), ethyl bromoacetate (1 eq.), acetone, r.t., 6 h, 100% b) 1 N aqueous NaOH (1.5 eq.), THF/EtOH 3:1, r.t., 6 h, 80% c) 4-benzylpiperidine or 1-benzylpiperazine (1 eq.), EDC HCl (1 eq.), HOBt (1 eq.), DMF, r.t., 6 h, 92% yield (for 14a) and 48% yield (for 14b). d) $LiAlH_4$ (1.5 eq.), dry THF, Ar, r.t., overnight, 9% yield (for 3a) and 50% yield (for 3b).

using pTSA as a catalyst and the Dean-Stark apparatus to trap the forming water, to give 1,5-dioxaspiro[5.5]undecane (**15**) [58]. By treating **15** with $AlCl_3$ and $LiAlH_4$, the acetal was selectively opened to 3-(cyclohexyloxy)propan-1-ol (**16**) in 91% yield (Scheme 4). Alcohol **16** was then converted to the corresponding chloride (**17**) by refluxing thionyl chloride in the presence of DMF as a catalyst. **17** was finally reacted with 1-benzylpiperazine or 4-benzylpiperidine to give the amines **4a-b**, as previously described (Scheme 4).

Compounds **5a-b** were prepared adopting the same synthetic approach previously described for the synthesis of **1a-b** (Scheme 5). The bromopropylthioether **18** was obtained by S_N2 between thiophenol and 1,3-dibromopropane in acetone at room temperature for 4 h, using K_2CO_3 as a base, and then directly reacted with 1-benzylpiperazine or 4-benzylpiperidine to give the amines **5a-b**, using the same reaction conditions previously reported (Scheme 5).

Final products **6a-b** were synthesized as reported in Scheme 6. Briefly, intermediate **20** was prepared by reduction of ethyl phenoxyacetate (**19**) with $NaBH_4$ in ethanol at room temperature for 4 h **19** was prepared by S_N2 reaction between phenol and ethyl bromoacetate in acetone at 60 °C for 4 h, using K_2CO_3 as base [57]. A total yield of 42% was achieved over the two steps (Scheme 6), compared to the 29% yield obtained in the single step reaction between phenol and 2-bromoethanol. **20** was chlorinated by refluxing thionyl chloride, using DMF as catalyst, to give 2-phenoxy-1-chloroethane (**21**), which was finally reacted with 1-benzylpiperazine or 4-benzylpiperidine to give the amines **6a-b** (Scheme 6).

For the synthesis of the phenyl ethyl thioether derivatives **7a-b**, the same approach adopted for compounds **3a-b** was followed (Scheme 7). Ethyl 2-(phenylsulfanyl)acetate (**22**) was prepared by S_N2 reaction between thiophenol and ethyl bromoacetate in acetone, with K_2CO_3 as base, at room temperature for 4 h. The ethyl ester was then hydrolysed in mild conditions using stoichiometric 1 N aqueous NaOH in THF/EtOH

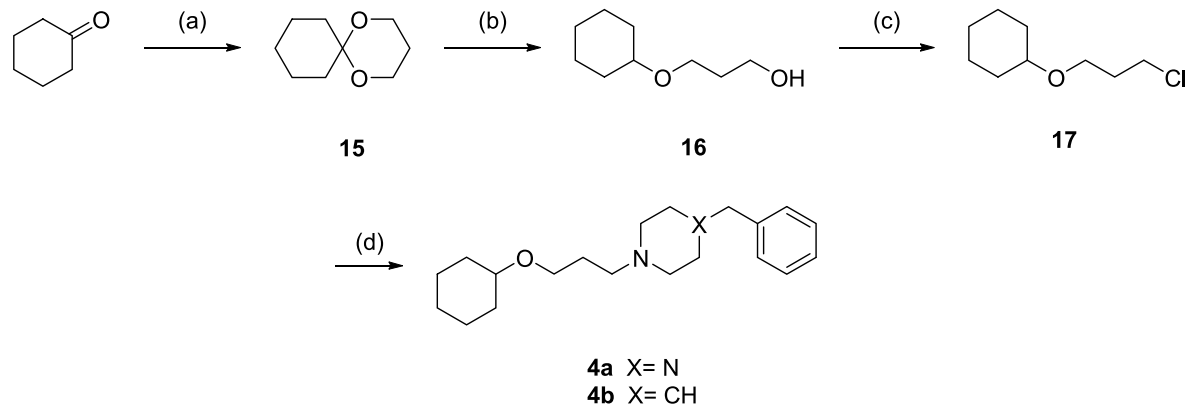

Scheme 4. Reagents and conditions: a) 1,3-propanediol (1.5 eq.), pTSA (0.1 eq.), dry toluene, reflux, N_2 atmosphere, 2 h, 35% b) $AlCl_3$ (2 eq.), $LiAlH_4$ (0.5 eq.), dry Et_2O, 0 °C → r.t. → 0 °C, 40′, 91% c) $SOCl_2$, neat, reflux, 4 h 78% d) 4-benzylpiperine or 1-benzylpiperazine (1.2 eq.), K_2CO_3 (2.5 eq.) DMSO, r.t., 36 h, 56% yield (for 4a) and 23% yield (for 4b).

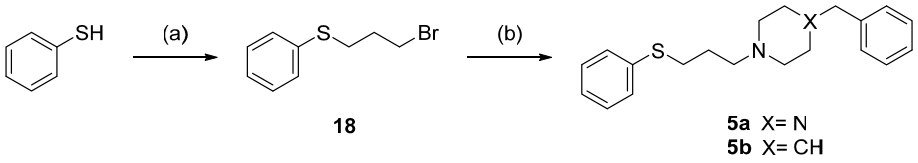

Scheme 5. Reagents and conditions: a) 1,3-Dibromopropane (3 eq.) and K_2CO_3 (1.5 eq.), Acetone, r.t., 4 h, 33% yield. b) 4-benzylpiperine or 1-benzylpiperazine (1.2 eq.), K_2CO_3 (2.5 eq.), DMSO, r.t., 6–48 h, 56% yield (for 5a) and 68% yield (for 5b).

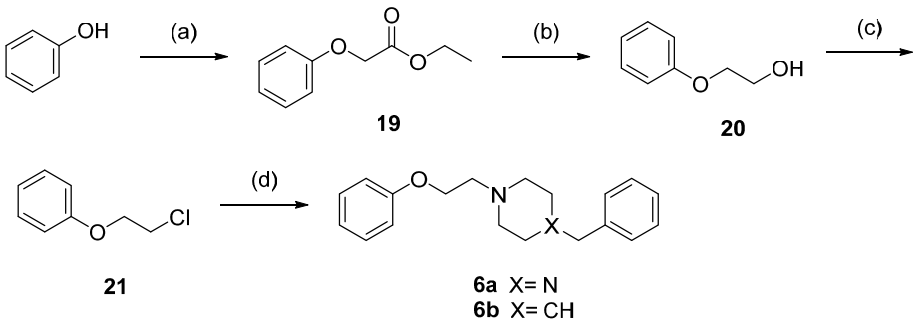

Scheme 6. Reagents and conditions: a) K_2CO_3 (2.5 eq.), ethyl bromoacetate (1 eq.), acetone, r.t. → 60 °C, 4 h, 52% b) $NaBH_4$ (1.5 eq.) in EtOH, r.t., 4 h, 80% c) $SOCl_2$, neat, reflux, 2 h, 67% d) 4-benzylpiperidine (1.2 eq.) or 1-benzylpiperazine (1.2 eq.), K_2CO_3 (2.5 eq.), DMSO, r.t., 24 h, 66% yield (for 6a) and 53% yield (for 6b).

3:1, at room temperature for 3 h, to give the free carboxylic acid **23.23** was coupled with 1-benzylpiperazine or 4-benzylpiperidine, using EDC and HOBt as coupling agents in DMF at 0 °C for 1 h and then at room temperature overnight, to yield the amides **24a** and **24b**, respectively. Reduction of the amides **24a-b** with $LiAlH_4$ in THF, at room temperature, overnight, afforded the corresponding amines **7a-b** in 55% and 60% yield, respectively.

Lastly, compounds **8a-b** were easily prepared as reported in Scheme 8, using the same approach described for the synthesis of **1a-b**. Phenol was reacted with an excess of 1,3-dibromopropane in DMF at room temperature overnight to give the product of mono-substitution **25**, that by reaction with 1-benzylpiperazine or 4-benzylpiperidine in DMSO at room temperature, gave amines **8a** and **8b** respectively (Scheme 8).

2.3. Binding assays

Compounds **1a-8a** and **1b-8b** were evaluated for binding affinity toward S1R and S2R in a radioligand displacement assay. Haloperidol was used as control compound in both assays. A primary screening at single concentration was performed first to profile the overall binding of the synthesized compounds at both S1R and S2R. The % of binding of the compounds (tested at 25 nM) are reported in **Tables SI–2.** Compounds **1a, 4a, 7a, 6b** and **8b**, which showed the highest % of binding at S1R (>95% at 25 nM) in the primary screening were assessed for binding at *h*NMDAR as well. We planned to assess the binding of selected S1R ligands at NMDAR, since it has been proposed that at high doses S1R agonists can cross-react with NMDARs and eventually block ion channel conductance, thus compromising the S1R-mediated neuroprotective

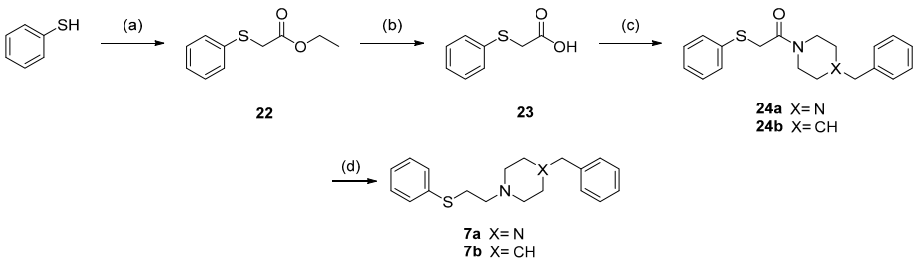

Scheme 7. Reagents and conditions: a) K_2CO_3 (2.5 eq), ethyl bromoacetate (1 eq.), acetone, r.t., 4 h, 65%. b) 1 N aqueous NaOH (1.5 eq.), THF/EtOH 3:1, r.t., 3 h, 72%. c) 4-benzylpiperidine or 1-benzylpiperazine (1 eq.), EDC HCl (1 eq.), HOBt (1 eq.), DMF, r.t., 24–48 h, 38% yield (for 24a) and 83% yield (for 24b). d) $LiAlH_4$ (1.5 eq.), dry THF, Argon, r.t., overnight, 23% yield (for 7a) and 88% yield (for 7b).

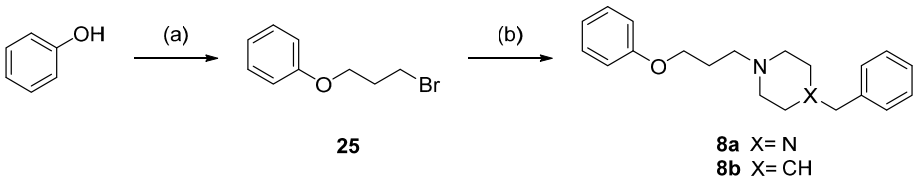

Scheme 8. Reagents and conditions: a) 1,3-dibromopropane (2 eq.) and K_2CO_3 (2.5 eq.), DMF, r.t., overnight, 73% yield. b) 4-benzylpiperine or 1-benzylpiperazine (1.2 eq.), K_2CO_3 (2.5 eq.), DMSO, r.t., 3–18 h, 56% yield (for 8a) and 49% yield (for 8b).

activity [46]. For this reason, it is necessary to have highly selective S1R agonist, without activity towards NMDAR, as neuroprotective agents. The five compounds were tested at 25 nM (the same concentration assessed in the primary screening at S1R and S2R) and the % of binding was calculated as % of displacement of the binding of the radiolabelled NMDAR antagonist CG19755. As showed in **Tables SI–3**, none of the tested compounds resulted effective NMDAR ligands, with % of binding <11.9% at the tested concentrations. Based on the results of the primary screening and considering that the aim of the work was to find out potent S1R ligands with low affinity towards S2R, we focused our attention on compounds **6b** and **8b**, for which the percentage of binding at S1R and S2R suggested a potential selectivity profile more shifted towards S1R. Therefore, for compounds **6b** and **8b** the binding affinities (K_i) was determined (**Figs. SI–1**). In detail, compound **6b** showed sub-nanomolar affinity toward S1R (K_i = 0.93 ± 0.06 nM) and low nanomolar affinity for S2R (K_i = 72 ± 1.4 nM), resulting in a 77-fold higher activity against the S1R subtype. A comparable binding profile was observed for compound **8b** with a S1R K_i = 1.1 ± 0.8 nM, S2R K_i = 88 ± 3.5 nM, and a S1R over S2R selectivity = 80.

2.4. Profiling the functional activity of selective S1R ligands

According to their low nanomolar affinity at S1R and their selectivity over S2R, compounds **6b** and **8b** were chosen for further investigation of the biological profile. The functional S1R activity of **6b** and **8b** was determined by evaluating their capability to enhance the neurite outgrowth induced by the nerve growth factor (NGF) in PC12 cells [26,27,59]. Before proceeding with the assay, the cytotoxicity of the tested compounds on PC12 cell lines was determined first, in order to define the optimal concentration range for subsequent experiments. An MTT-based cytotoxicity assay, performed after treating PC12 cells with **6b** and **8b** did not show remarkable cytotoxicity at concentration <1 μM and < 5 μM, respectively, thus confirming that both compounds are nontoxic at the concentration used in our NGF-induced neurite outgrowth experiments (data not shown). Accordingly, in the neurite outgrowth assay (Fig. 6), **6b** and **8b** were tested up to 5 μM. *(R)*-RC-33

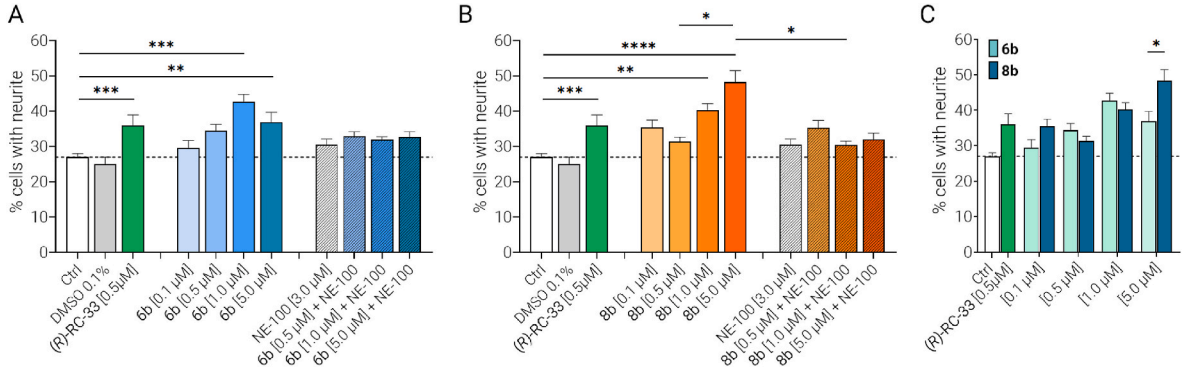

Fig. 6. Quantification of the neurite outgrowth in PC12 cells exposed to NGF and treated with compounds **6b** (A) and **8b** (B) alone or pre-treated with the S1R antagonist NE-100 (at 3 μM). The neurite outgrowth induced by *(R)*-RC-33, used as reference compound, has been included for comparison. (C) Comparison of the neurite outgrowth after treatment with compound **6b** and **8b**. Each bar represents the percentage of cells with neurite sprout. The results are expressed as mean ± SEM of three independent experiments. *p < 0.05; **p < 0.01; ***p < 0.001; ****p < 0.0001 determined by Kruskal Wallis followed by Dunn's post-hoc test.

(Fig. 6 and **SI-2**), our in house potent S1R agonist, was used as reference compound in all assays and the results are in line with those reported in our previous work. *(R)*-RC-33 is a potent and selective S1R agonist fully characterized for its affinity, activity, potency, toxicity, stability, PK properties, CNS distribution and neuroprotective properties [26,27,34,38,60,61]. NGF alone promoted the neurite sprouting in 26 ± 4% of PC12 cells at 2.5 nM, whereas *(R)*-RC-33 was able to promote the neurite outgrowth in the 36 ± 4% of PC12 cells at 0.5 μM compared to the control. As shown in Fig. 6A–C (and in **Figs. SI–3**), both compounds **6b** and **8b** significantly increased the NGF induced neurite outgrowth at all the tested concentrations in a dose-dependent manner and with a similar profile. In detail, **6b** promoted the neuritis differentiation starting from the concentration of 0.5 μM (37 ± 5%) with a maximum differentiation effect observed at 1 μM. Conversely, **8b** showed an undeniable effect in favouring the neurite growth already at 0.1 μM with a more pronounced dose-response profile, suggesting a greater potency for **8b** compared to **6b**. It has to be underlined that for both compounds binding affinity values are in the nanomolar range, while in neurite outgrowth assay they are active in submicromolar range. A similar trend was already observed for RC-33 and PRE-084, another well-known and characterized S1R agonist [60–62]. Moreover, similarly to RC-33, the neurite outgrowth induced by **6b** and **8b** was reverted by the coincubation with NE-100, thus confirming a S1R agonist profile for both compounds **6b** and **8b**.

2.5. Neuroprotective capacity of *6b* and *8b*

The capacity of the selected compounds **6b** and **8b** to protect neurons from the degenerative damage induced by toxic insults (e.g., the oxidative stress induced by rotenone and oligomycin and the excitotoxic stress induced by NMDA) was evaluated *in-vitro*. Compound **II**, endowed with neuroprotective activity against rotenone, oligomycin and NMDA cytotoxic insults, was used as reference compound, and the results are in line with our previously reported data [51]. ROS are normally produced in neurons. However, the alteration of mitochondrial function and the consequent increase in oxidative stress start at the early stages of neurodegeneration, prior to neuronal cell death. Rotenone and oligomycin are inhibitors of the mitochondrial complex I and the mitochondrial membrane-bound ATP synthase, respectively, thus causing a massive energetic impairment and overproduction of ROS [63–66]. Differentiated SH-SY5Y cells are useful in vitro models to investigate bioenergetic alterations in mitochondrial dysfunction-related pathologies such as neurodegenerative diseases [67,68]. Thus, the capability of compounds **6b** and **8b** to protect SH-SY5Y cells from oxidative damage induced by rotenone and oligomycin via S1R activation was evaluated. First, the cytotoxicity of **6b** and **8b** was assessed on SH-SY5Y cell line at six concentrations (from 0.1 to 100 μM) in order to determine the optimal doses for neuroprotective studies. The results, expressed as percentage of cell viability after 72 h of incubation, are reported in **Figs. SI–4**. In particular, both compounds showed a good safety profile with no significant cell death (vs. control) at lower concentrations (from 0.1 to 50 μM), whereas a modest cytotoxicity (% of cell viability of 76% and 82% for **6b** and **8b** , respectively) was observed at the highest dose of 100 μM. The neuroprotective capacity of **6b** and **8b** was evaluated at concentrations of 1 and 5 μM, corresponding to the efficacy doses for neuritis outgrowth, and was reported as percentage of cell viability of SH-SY5Y cells after treatment with the compound in the presence of the toxic stimuli. As reported in Fig. 7, both **6b** and **8b** were able to significantly prevent cell damage induced by rotenone when tested at the concentration of 1 μM, with a % of cell viability of 65% and 68%, respectively. To investigate the role of S1R in this process, the neuroprotective activity of the two compounds were tested by pre-treating SH-SY5Y cells with 5 μM of PB212, an in-house developed S1R antagonist [69]. Both **6b** and **8b**, at 1 μM, displayed a significant decrease of their neuroprotective capacity in combination with PB212 thus supporting a S1R mediated neuroprotective mechanism.

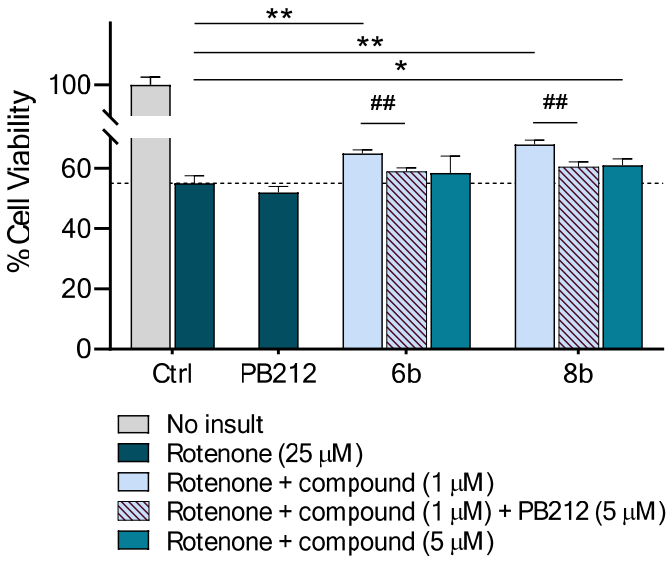

Fig. 7. Neuroprotective effect, expressed as % of cell viability (SH-SY5Y cells), of the tested compounds **6b** and **8b** at 1.0 and 5.0 μM in the presence of rotenone (25 μM) and a combination of rotenone and the S1R antagonist, PB212 (5 μM). Each bar represents the mean ± SD of three independent experiments: *p < 0.1; **p < 0.01; ##p < 0.01.

Conversely, no neuroprotective capacity for **6b** and **8b** was observed when oligomycin (at 2.5 μM) was used as a toxic stimulus (**Figs. SI–5**). Compound **6b** and **8b** were also tested to assess their neuroprotective potential against NMDA-induced neuro- and excitotoxicity. The results are reported in Fig. 8A. Briefly, neuroblastoma cells were incubated for 24 h in the presence of NMDA at 250 μM (corresponding to its CC_{50}, **Tables SI–4**) and four different concentrations of **6b** and **8b** (ranging from 0.1 to 5 μM). Memantine, a non-competitive NMDAR antagonist, used in clinic to slow the progression of moderate-to-severe AD [51,70], was used as positive control and reference drug for comparing the anti-glutamatergic activity of the compounds.

The tested compounds demonstrated a neuroprotective effect against NMDA stimuli with a complete cell survival at all four tested concentrations (Fig. 8A). It is worthy to point out that the two compounds showed an efficacy comparable to memantine at the lowest doses (0.1 and 0.5 μM) but superior at the higher doses of 1 and 5 μM. Indeed, the neuroprotective capacity of memantine decreases with increasing concentration, resulting completely ineffective at 5 μM. The bell-shape behaviour observed for memantine could be due to the slightly higher cytotoxicity of the drug against SH-SY5Y cells. Memantine showed an CC_{50} of 98 μM, with 70% of cell viability when assessed at the 5 μM (the same maximum concentration exploited in the neuroprotective assay, **Figs. SI–4** and **Tables SI–4**). Conversely, compounds **6b** and **8b** did not show any cytotoxicity at the neuroprotective assay concentrations, and a hint of cytotoxicity was only observed when assessed at 100 μM (% of cell viability around 80%). Thus, compounds **6b** and **8b** presented a superior efficacy/toxicity profile than memantine. To further demonstrate the involvement of SRs in their neuroprotective effects against NMDA excitotoxicity, compounds **6b** and **8b** were assessed in the presence of the S1R antagonist PB212. The neuroprotective activity of both **6b** and **8b** was significantly reverted by the presence of the S1R antagonist (Fig. 8B), thus confirming their agonist profile. To sum up, both compounds **6b** and **8b** showed a good neuroprotective profile in all the performed experiments and therefor they will be further investigated for their developability profile.

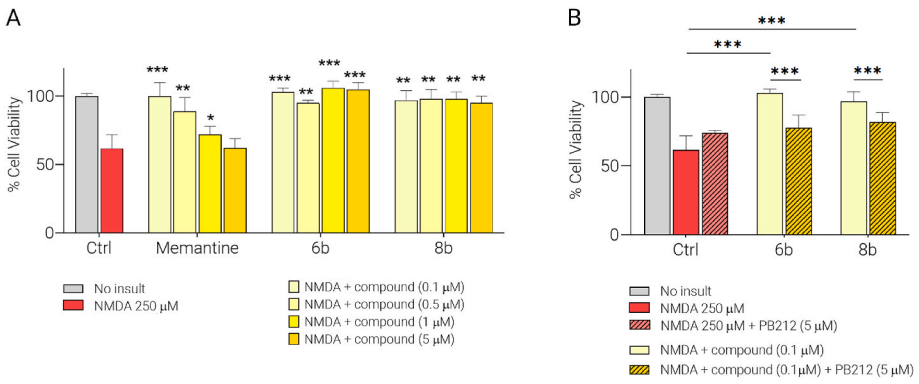

Fig. 8. (A) Neuroprotective effect expressed as % of cell viability (SHSY5Y cells) of compounds **6b**, **8b** and memantine (used as reference drug) at four concentration (0.1–5 μM) against 250 μM NMDA-induced cytotoxicity in SH-SY5Y neuroblastoma cells. (B) Neuroprotective effect of compounds **6b** and **8b** (0.1 μM) in the presence of NMDA (250 μM) and a combination of NMDA and PB212 (5 μM). Cell viability was assessed by MTT test. Each bar represents the mean ± SD of three independent experiments; *p < 0,1; **p < 0,01; ***p < 0,001.

2.6. *In vitro and in vivo toxicity studies*

Ascertained the potential of **6b** and **8b** as neuroprotective agents, early toxicity studies were performed with the aim to identify liabilities and to select the safest compounds for progression toward further studies. Early toxicity assays included in vitro cytotoxicity against three human cell lines that overexpress both S1R and S2R genes (SIGMA1 and TMEM97, respectively, Fig. 9), namely A549 (human lung adenocarcinoma epithelial cells), LoVo (colorectal cancer cells) and Panc-1 (pancreatic cancer cells).

Cell lines A549, LoVo and Panc-1 were exposed for 24, 48 and 72 h to increasing concentration of compounds **6b** and **8b**. IC_{50} value was not reached at none of the concentrations of both compounds tested. Nevertheless, after 48 h and 72 h, either **6b** and **8b** reduced of 20% and 40% of Panc-1 and LoVo cells survival, respectively, at the highest concentration of 100 μM (Fig. 10), whereas no cytotoxicity was observed at concentrations ≤10 μM to which the compounds showed the greatest neuroprotective activity.

Water solubility is an essential requirement for developing effective drugs with a proper druggability profile and should be considered before proceeding in vivo studies. The thermodynamic solubilities of compounds **6b** and **8b** was measured at three key physiological pH values (pH 1.2 gastric environment, pH 6.8 small intestine, and pH 7.4 plasma) [71,72]. The results are reported in **Tables SI–5**. Briefly, compound **6b** and **8b** showed a solubility in the range of 7.8–8.6 mg/mL and of 2.8–3.0 mg/mL in all the three assessed buffers, respectively. The lack of significative differences in the solubility of each compound at the three pH values is justified by a comparable distribution of the dissociated and undissociated microspecies at pH 1.2, 6.8 and 7.4, according with the pK_a value of the basic amine (pK_a 8.56 and 9.26 for compounds **6b** and **8b**, respectively; **Tables SI–1**). The slight less solubility of **8b**, compared to **6b**, agrees with the slender higher hydrophobicity of the former compound (log*P* = 3.997 and 4.375 for compounds **6b** and **8b**, respectively; **Tables SI–1**). Nevertheless, according to the solubility category classification of the USP, both compounds could be considered as slightly soluble but suitable for in vivo assay, and they are in line with the solubility requirement for CNS directed compounds [54,73,74].

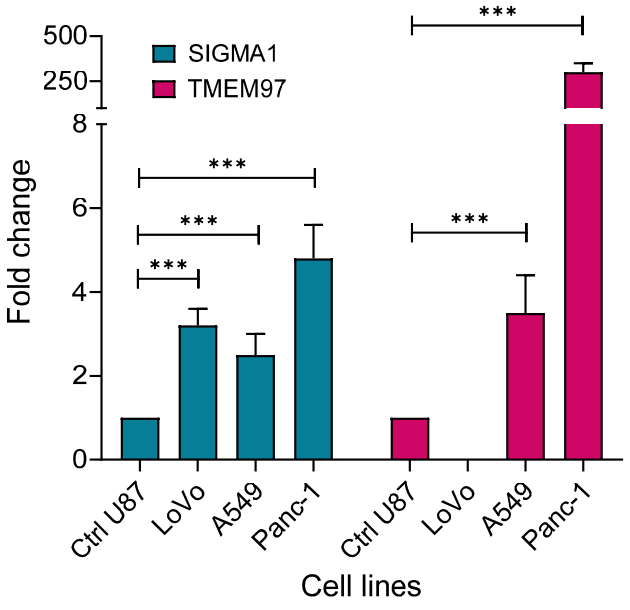

Fig. 9. Gene expression profile for S1R (SIGMA1) and S2R (TMEM97) in LoVo, A549 and Panc-1 cell lines. The results are expressed as fold change with the respect of the gene expression in U87 cell lines, assumed as reference. Data are reported as mean ± SD. *** = p < 0.001.

The *in-vivo* toxicity was then evaluated, using the predictive zebrafish animal model. The cell structural and biochemical similarities between humans and zebrafish enable rapid forecasting of the possible impacts of chemical and other substances on health human being. The zebrafish is a suitable model for screening drugs for potential toxicity on the nervous, cardiovascular, and digestive systems [75]. Numerous studies confirmed that mammalian and zebrafish toxicity profiles are strikingly similar, and zebrafish usually can serve as an intermediate step between cell-based evaluation and conventional animal testing [76]. Zebrafish embryos were exposed to increasing concentration (from 0.1 to 50 μM) of compounds **6b** and **8b** immediately after eggs' fertilization. The mortality rate and the kind of developmental deficiencies were evaluated 5 days-post-fertilisations. As reported in Fig. 11A, a slight dose-dependent toxicity on zebrafish embryos was observed for both compounds. All embryos exposed to the lowest concentrations of both **6b** and **8b** (0.1 μM and 1 μM) showed a normal and vital phenotype compared to the control. Decrease in the embryo vitality rate and increase in the entity of damages to vital structures became more evident at higher concentrations (Fig. 11A, **Table SI-6-7**). At the concentration of 10 μM, **6b** induced the death of 4 embryos out of 8. Moreover, among the living embryos, morphological abnormalities mainly affecting the shape of tail, heart and skin pigmentation were observed (Fig. 11B–E). In particular, embryos showed short and up-curved tail, an enlarged volume of heart, and poor pigmentation (**Figs. SI–6**). Furthermore, the swim bladder was not well inflated, and oedema was evident. Notably, 75% of live embryos showed a coiled tail and 100% exhibited a variable expanded heart volume. Conversely, **8b** did not induce embryo death (100% of embryos alive) at 10 μM, with just one exemplar showing enlarged volume of heart and a slightly coiling shape. Lastly, both compounds induced the death of all zebrafish embryo at the highest dose tested (50 μM).

Compound **6b** at low concentrations (1 μM) caused a minimal variation in morphology (score 4) related to a potentially recoverable developmental delay or anomaly [77] and induced severe and multiple

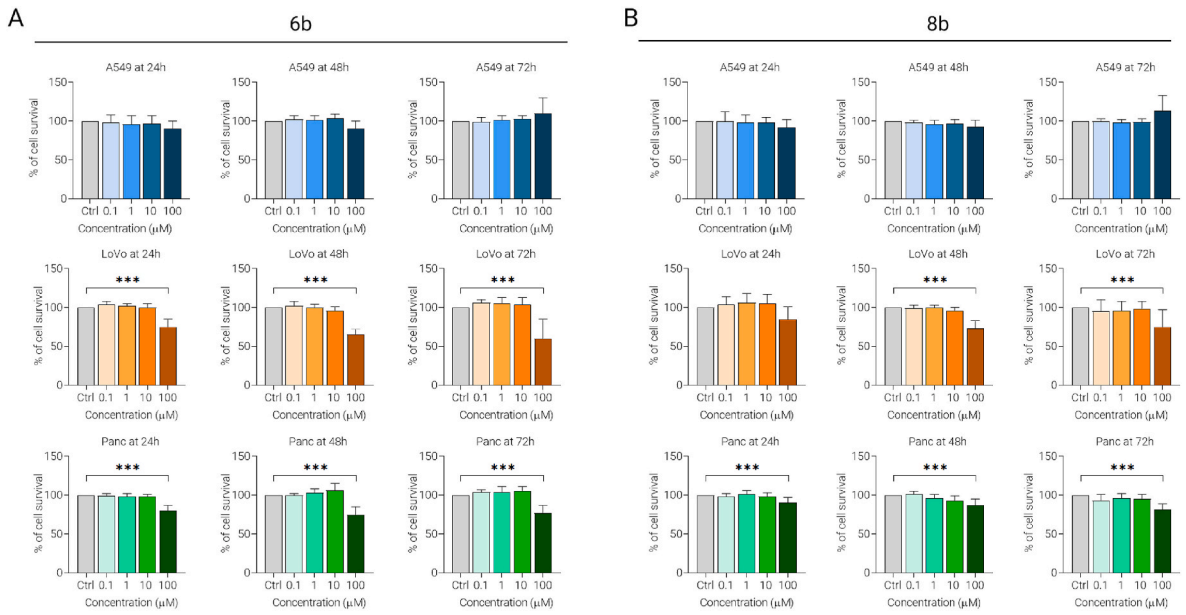

Fig. 10. Cytotoxicity evaluation (expressed as % of cell survival) for compounds **6b** (A) and **8b** (B) against A549, LoVo and Panc-1 cancer cell lines. Cell survival was evaluated at 0.1, 1, 10, 100 μM at 24, 48, 72 h after exposure. Data are reported as mean ± SD. *** = $p < 0.0001$.

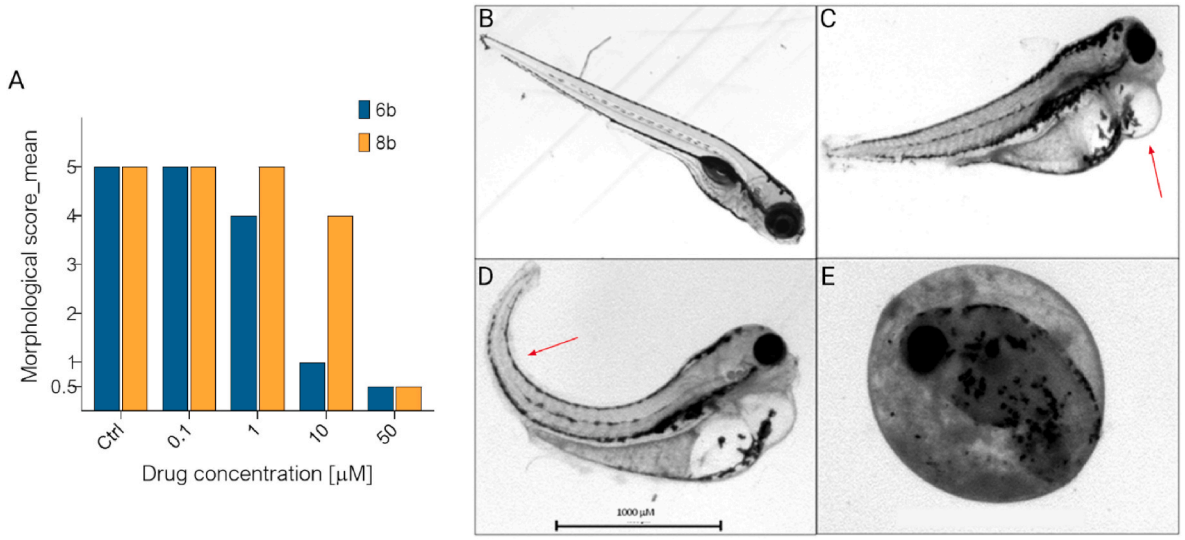

Fig. 11. Morphological score (A) obtained from the average values of the sample score sheet (Tables SI–X) and representative body shape morphology of zebrafishes observed during treatment with high dose of compounds **6b** and **8b:** normal body shape (B); abnormal hearth morphology: heart severely enlarged (C); abnormal body shape: severely curved tail (D); abnormal development: embryo died before complete development (E). The main morphological alteration observed are pointed with a red arrow. Exposure time: 120 h, 5 days-post-fertilization.

malformations (score 1) only at 10 μM. It showed a low toxicity profile at concentration < 10 μM. Conversely, compound **8b** did not cause evident (score 5) or slight alteration (score 4) of anatomical structures, at 1 μM or 10 μM, respectively. To sum up, the results of in vivo model suggest a very low toxicity profile of both compounds at the doses employed for neuroprotective effects (i.e., <10 μM).

3. Conclusion

It is well established that S1R plays a role in neuroprotection by preventing the NMDA-mediated excitotoxicity and ROS-induced oxidative stress. In the present work, we reported the identification of a new series of S1R ligands endowed with potential neuroprotective properties. The compounds were designed according to a ring opening approach applied to our previously identified S1R ligand **II** which showed S1R-mediated neuroprotective capacity. Compounds **6b** and **8b** stand out for their high affinity for S1R (*Ki* = 0.93 nM and 1.1 nM, respectively), and selectivity over S2R (S1R over S2R selectivity >77-fold). Functional assay revealed a S1R agonists profile for both compounds since they were able to enhance the neurite outgrowth induced by nerve growth factor (NGF) in PC12 cell lines. **6b** and **8b** exhibited neuroprotective effects against rotenone- and NMDA-induced neurotoxicity in SH-SY5Y neuroblastoma cell lines. The neuroprotective effect was reverted by co-treatment with PB212, a S1R antagonist. Moreover, **6b** and **8b** showed an efficacy and safety profile comparable or superior to memantine, a NMDA uncompetitive antagonist used as reference drug. Conversely to memantine, both compounds did not show to bind NMDAR, thus confirming a S1R-mediated neuroprotection activity.

Interestingly, having highly selective and potent S1R agonists, without activity against NMDAR, seems to be pivotal for the development of S1R agonists with neuroprotective activity against glutamate-excitotoxicity. Indeed, several studies revealed that S1R agonists able to cross-react with NMDARs causing the block of the ion channel conductance do not result in the beneficial neuroprotective effect [78–80]. Cytotoxicity (performed in vitro on SH-SY5Y, A549, LoVo and Panc-1 cell lines) and in vivo toxicity assay (performed in the zebrafish model) suggested a very low toxicity profile for both compounds. To sum up, the data obtained thus far, clearly prove the potential of the N-(phenoxyalkyl) benzylpiperidine scaffold in the development of selective, safe, but most importantly effective S1R agonists endowed with neuroprotective activity on neuronal cells against toxic insults responsible for the development of neurodegenerative diseases. The efficacy and null toxicity for **6b** and **8b** at the concentrations useful for obtaining neuroprotective effects thus encourage further preclinical investigation on in vivo neurodegenerative models.

4. Experimental section

4.1. Chemistry

All commercially available chemicals and solvents were of reagent grade and were used without further purification unless otherwise specified. The following solvents and reagents have been abbreviated: 1-ethyl-3-(3-dimethylaminopropyl) carbodiimide (EDC); cyclohexane (CE); dichloromethane (DCM); diethyl ether (Et_2O); dimethyl sulfoxide (DMSO); dimethylformamide (DMF); ethanol (EtOH); ethyl acetate (AcOEt); hydroxy benzotriazole (HOBt); methanol (MeOH); *p*-toluene sulfonic acid (pTSA); piperazine (ppz); piperidine (ppd); tetrahydrofuran (THF); Thiophenol (Thioph). Reactions were monitored by thin-layer chromatography on silica gel plates (60F-254, E. Merck) and visualized with UV light, cerium ammonium sulfate or alkaline $KMnO_4$ aqueous solution. NMR spectra were recorded on a Bruker 400 spectrometer with ^1H at 400.134 MHz and ^{13}C at 100.62 MHz. Proton chemical shifts were referenced to the solvent residual peaks. Chemical shifts are reported in parts per million (ppm, δ units). Coupling constants are reported in hertz (Hz). Splitting patterns are designed as s, singlet; d, doublet; t, triplet; q quartet; dd, double doublet; ddd, doublet of doublet of doublets; dddd, doublet of doublet of doublet of doublets; dt, double of triplets; m, multiplet; b, broad. Purity of compounds 6b and 8b was assessed by UPLC-UV-ESI/MS. Analyses were run on a ACQUITY BEH Phenyl (ABP) (50 × 2.1 mm, 1.7 μm particle size) column, at r.t., in isocratic elution (solvent A: water containing 0.1% of formic acid; solvent B: methanol containing 0.1% of formic acid; mobile phase 70% of B) at a flow rate of 1 mL min−1. The chromatograms were recorded at 265 nm wavelength. All the final compounds had 95% or higher purity.

4.1.1. Synthesis of ethyl 2-phenoxyacetate (19)

To a solution of phenol (1.0 g, 10.6 mmol, 1.1 eq.) in DMF (5 mL), K_2CO_3 (3340 mg, 24.15 mmol, 2.5 eq.) was added and the suspension was stirred at room temperature for 30 min. Thereafter, ethyl-bromoacetate (1.068 mL, 9.66 mmol, 1 eq.) was added and the mixture stirred at 60 °C for 4 h. The reaction was chilled at room temperature, diluted with AcOEt, and sequentially washed with water, 1 N aqueous NaOH and brine. The organic layer was dried over anhydrous Na_2SO_4 and concentrated to give 906 mg (52% yield) of a colorless liquid, which was pure enough to be used in the next step without further purification. ^1H NMR (400 MHz, $CDCl_3$) δ 7.31 (dt, J = 8.3, 6.9 Hz, 2H, C$\underline{H}_{Phen}$-3, 5), 7.02 (t, J = 7.4 Hz, 1H, C$\underline{H}_{Phen}$-4), 6.94 (d, J = 7.9 Hz, 2H, C$\underline{H}_{phen}$-2, 6), 4.64 (s, 2H, C$\underline{H}_2$OPh), 4.30 (q, J = 7.1 Hz, 2H, COOC$\underline{H}_2$), 1.32 (t, J = 7.1 Hz, 3H, COOCH$_2$C$\underline{H}_3$).

4.1.2. Synthesis of 2-phenoxyethan-1-ol (20)

To a solution of 2-phenoxyacetate (906 mg, 5.03 mmol, 1 eq.) in EtOH (5 mL), $NaBH_4$ (285 mg, 7.55 mmol, 1.5 eq.) was added and the suspension was stirred at room temperature for 4 h. The suspension was filtered, and the filtrate was diluted with water and extracted with AcOEt. The organic layer was dried over anhydrous Na_2SO_4 and concentrated to give 557 mg (80% yield) of a colorless oil, which was pure enough to be used in the next step without further purification. ^1H NMR (400 MHz, $CDCl_3$) δ 7.32 (ddd, J = 14.5, 9.8, 4.5 Hz, 2H, C$\underline{H}_{Ar}$-3,5), 7.03–6.91 (m, 3H, C$\underline{H}_{Ar}$-2,4,6), 4.13–4.09 (m, 2H, C$\underline{H}_2$OPh), 4.01–3.97 (m, 2H, C$\underline{H}_2$OH).

4.1.3. Synthesis of (2-chloroethoxy)benzene (21)

2-phenoxyethan-1-ol (200 mg, 1.45 mmol, 1 eq.) was solubilized in 5 mL of $SOCl_2$ and stirred at 60 °C for 2 h. The solvent was evaporated under reduced pressure. The residue was chilled at room temperature, diluted with AcOEt, and washed with a saturated solution of $NaHCO_3$ and brine. The organic layer was dried over anhydrous Na_2SO_4 and concentrated to give 211 mg of a crude that was purified by column chromatography (crude:silica gel 1:100; mobile phase: CE:AcOEt 9:1) to give 150 mg of a yellow oil (66% yield). ^1H NMR (400 MHz, $CDCl_3$) δ 7.36–7.30 (m, 2H, C$\underline{H}_{Ar}$-3,5), 7.01 (t, J = 7.4 Hz, 1H, C$\underline{H}_{Ar}$-4), 6.95 (d, J = 7.9 Hz, 2H, C$\underline{H}_{Ar}$-2,6), 4.26 (t, J = 6.0 Hz, 2H, C$\underline{H}_2$OPh), 3.84 (t, J = 6.0 Hz, 2H, C$\underline{H}_2$Cl).

4.1.4. General procedure for the synthesis of ethyl cyclohexanetiol/thiofenol acetates 12 and 22

To a solution of cyclohexanethiol or thiophenol (1 eq.) in acetone (5 mL), K_2CO_3 (2.5 eq.) was added, and the suspension was stirred at room temperature for 30 min. Thereafter, ethyl 2-bromoacetate (1 eq.) was added and the mixture was stirred at room temperature for 4–6 h. Thereafter, the reaction was diluted with AcOEt and washed with saturated solution of Na_2CO_3. The organic layer was dried over anhydrous Na_2SO_4 and concentrated, to give the title compounds, pure enough to be used in the next step without further purification.

4.1.4.1. Ethyl 2-(cyclohexylsulfanyl)acetate (12). Colorless liquid, 1.74g (quantitative yield). ^1H NMR (400 MHz, $CDCl_3$) δ 4.18 (q, J = 7.1 Hz, 2H, COOC$\underline{H}_2$CH$_3$), 3.23 (s, 2H, CyhexSC$\underline{H}_2$), 2.84–2.74 (m, 1H, C$\underline{H}$-1-cyhex), 2.03–1.92 (m, 2H, C$\underline{H}$-2-cyhex, C$\underline{H}$-6-cyhex), 1.80–1.70 (m, 2H, C$\underline{H}$-2′-cyhex, C$\underline{H}$-6′-cyhex), 1.66–1.55 (m, 1H, C$\underline{H}$-4-cyhex), 1.38–1.17 (m, 8H, C$\underline{H}_2$-3-cyhex, C$\underline{H}_2$-5-cyhex, C$\underline{H}$-4′-cyhex, COOCH$_2$C$\underline{H}_3$). ^{13}C NMR (101 MHz, $CDCl_3$) δ 170.91 (C$\underline{O}$O), 61.24 (COOC$\underline{H}_2$CH$_3$), 43.98 (C$\underline{H}$-1-cyhex), 33.10 (CyhexSC$\underline{H}_2$), 32.09 (C$\underline{H}_2$-2-cyhex, C$\underline{H}_2$-6-cyhex), 25.93 (C$\underline{H}_2$-4-cyhex), 25.74 (C$\underline{H}_2$-3-cyhex, C$\underline{H}_2$-5-cyhex), 14.15 (COOCH$_2$C$\underline{H}_3$).

4.1.4.2. Ethyl 2-(phenylsulfanyl)acetate (22). The product was purified by column chromatography (crude:silica gel: 1:50; CE:AcOEt 9:1) to give 1.143g of a colorless oil (64% yield). ^1H NMR (400 MHz, $CDCl_3$) δ 7.37–7.31 (m, 2H, C$\underline{H}_{Ar}$-2,6), 7.23 (t, J = 7.5 Hz, 2H, C$\underline{H}_{Ar}$-3,5), 7.20–7.14 (m, 1H, C$\underline{H}_{Ar}$-4), 4.09 (q, J = 7.1 Hz, 2H, COOC$\underline{H}_2$CH$_3$), 3.56 (s, 2H, SC$\underline{H}_2$COOH), 1.15 (t, J = 7.1 Hz, 3H, COOCH$_2$C$\underline{H}_3$). ^{13}C NMR (100 MHz, $CDCl_3$) δ 169.03 (C$\underline{O}$OCH$_2$), 135.10 (C$\underline{C}_{Ar}$-1), 129.70 (C$\underline{H}_{Ar}$-2,6), 129.03 (C$\underline{H}_{Ar}$-3,5), 126.58 (C$\underline{H}_{Ar}$-4), 61.73 (COOC$\underline{H}_2$), 35.60 (SC$\underline{H}_2$COO), 13.97 (COOCH$_2$C$\underline{H}_3$).

4.1.5. General procedure for the synthesis of cyclohexanetiol/thiofenol carboxylic acid 13 and 23

To a solution of carboxylic acid (1 eq.) in a solution of THF/EtOH 3:1 (10 mL), 1 N aqueous NaOH (1.5 eq.) was added, and the suspension was stirred at room temperature for 3–6 h. The reaction was quenched with water and acidified to pH 2 with 1 N aqueous HCl. The aqueous layer was extracted with AcOEt, and the organic phase dried over anhydrous Na_2SO_4. The crude product, pure enough, was used in the next step without further purification.

4.1.5.1. 2-(cyclohexylsulfanyl)acetic acid (13). Colorless liquid, 1.2 g

(80% yield). ^{1}H NMR (400 MHz, $CDCl_3$) δ 3.29 (s, 2H, CyhexSC$\underline{H}_2$), 2.87–2.79 (m, 1H, C$\underline{H}$-1-cyhex), 2.03–1.95 (m, 2H, C$\underline{H}$-2-cyhex, C$\underline{H}$-6-cyhex), 1.85–1.70 (m, 2H, C$\underline{H}$-2′-cyhex, C$\underline{H}$-6′-cyhex), 1.68–1.58 (m, 1H, C$\underline{H}$-4-cyhex), 1.43–1.18 (m, 5H, C$\underline{H}_2$-3-cyhex, C$\underline{H}$-4′-cyex, C$\underline{H}_2$-6-cyhex). ^{13}C NMR (101 MHz, $CDCl_3$) δ 176.52 (COOH), 44.10 (CH-1-cyhex), 33.00 (CyhexSC$\underline{H}_2$), 31.85 (C$\underline{H}_2$-2-cyhex, C$\underline{H}_2$-6-cyhex), 25.89 (C$\underline{H}_2$-4-cyhex), 25.70 (C$\underline{H}_2$-3-cyhex, C$\underline{H}_2$-5-cyhex).

4.1.5.2. 2-(phenylsulfanyl)acetic acid (23). White solid, 710 mg (72% yield). ^{1}H NMR (400 MHz, $CDCl_3$) δ 7.48–7.42 (m, 2H, C$\underline{H}_{Ar}$-2,6), 7.34 (dd, J = 10.1, 4.8 Hz, 2H, C$\underline{H}_{Ar}$-3,5), 7.31–7.24 (m, 1H, C$\underline{H}_{Ar}$-4), 3.70 (s, 2H, SC$\underline{H}_2$COOH). ^{13}C NMR (100 MHz, $CDCl_3$) δ 175.10 (COOH), 135.10 (C$\underline{C}_{Ar}$-1), 129.70 (C$\underline{H}_{Ar}$-2,6), 129.03 (C$\underline{H}_{Ar}$-3,5), 126.58 (C$\underline{H}_{Ar}$-4), 34.77 (S$\underline{C}H_2$COO).

4.1.6. General procedure for the synthesis of the amides 14a-b, 24a-b

To a solution of appropriate carboxylic acid 13 or 23 (1 eq.) in DMF (5 mL), EDC HCl (1 eq.), HOBt (1 eq.) and 4-benzylpiperidine or 1-benzylpiperazine (1 eq.) were added at 0 °C. The temperature was spontaneously raised to room temperature and the reaction was stirred in the same condition for 6–24 h. The mixture was diluted with AcOEt and sequentially washed with water, saturated solution of Na_2CO_3, saturated solution of NH_4Cl and brine. The organic layer was dried over anhydrous Na_2SO_4 and concentrated to afford the titled compounds.

4.1.6.1. 1-(4-Benzylpiperazin-1-yl)-2-(cyclohexylsulfanyl)ethan-1-one (14a). Yellow oil, 530 mg (93% yield). ^{1}H NMR (400 MHz, $CDCl_3$) δ 7.37–7.32 (m, 4H, C$\underline{H}_{Ar}$-2,3,5,6), 7.31–7.25 (m, 1H, C$\underline{H}_{Ar}$-4), 3.71–3.60 (m, 2H, C$\underline{H}$-2-ppz, C$\underline{H}$-6-ppz), 3.57–3.48 (m, 4H, C$\underline{H}_2$Bn, C$\underline{H}$-2′-ppz, C$\underline{H}$-6′-ppz), 3.34 (s, 2H, SC$\underline{H}_2$CO), 2.88–2.75 (m, 1H, C$\underline{H}$-1-cyhex), 2.53–2.40 (m, 4H, C$\underline{H}_2$-3-ppz, C$\underline{H}_2$-5-ppz), 2.12–1.96 (m, 2H, C$\underline{H}$-2-cyhex, C$\underline{H}$-6-cyhex), 1.77 (d, J = 3.4 Hz, 2H, C$\underline{H}$-3-cyhex, C$\underline{H}$-5-cyhex), 1.68–1.55 (m, 1H, C$\underline{H}$-4-cyhex), 1.29 (ddd, J = 17.0, 14.9, 6.9 Hz, 5H; C$\underline{H}$-2′-cyhex, C$\underline{H}$-3′-cyhex,C$\underline{H}$-4′-cyhex, C$\underline{H}$-5′-cyhex, C$\underline{H}$-6′-cyhex). ^{13}C NMR (101 MHz, $CDCl_3$) δ 168.39 (SC$\underline{H}_2$CON), 137.79 (C$\underline{C}_{Ar}$-1), 129.24 (C$\underline{H}_{Ar}$-2,6), 128.45 (C$\underline{H}_{Ar}$-4), 127.39 (C$\underline{H}_{Ar}$-3,5), 63.01 (C$\underline{H}_2$-2-ppz), 53.18 (C$\underline{H}_2$-6-ppz), 52.85 (C$\underline{H}_2$-3-ppz), 46.60 (C$\underline{H}_2$-5-ppz), 44.29 (C$\underline{H}_2$Bn), 41.98 (C$\underline{H}$-1-cyhex), 33.52 (SC$\underline{H}_2$CO), 32.14 (C$\underline{H}$-2-cyhex, C$\underline{H}$-6-cyhex), 26.06 (C$\underline{H}$-4-cyhex), 25.88 (C$\underline{H}$-3-cyhex, C$\underline{H}$-5-cyhex).

4.1.6.2. 1-(4-Benzylpiperidin-1-yl)-2-(cyclohexylsulfanyl)ethan-1-one (14b). The product was purified by column chromatography (crude: silica gel: 1:70; CE:AcOEt 1:1) to give 273 mg of a yellow oil (48% yield). ^{1}H NMR (400 MHz, $CDCl_3$) δ 7.31 (dd, J = 10.2, 4.6 Hz, 2H, C$\underline{H}_{Ar}$-3,5), 7.22 (dd, J = 8.4, 6.3 Hz, 1H, C$\underline{H}_{Ar}$-4), 7.18–7.13 (m, 2H, C$\underline{H}_{Ar}$-2,6), 4.62–4.52 (m, 1H, C$\underline{H}$-2- ppd), 3.91–3.80 (m, 1H, C$\underline{H}$-2′- ppd), 3,34 (s, 2H, CyhexSC$\underline{H}_2$), 3.00 (td, J = 13.3, 2.4 Hz, 1H, C$\underline{H}$-6- ppd), 2.82 (dq, J = 10.5, 3.6 Hz, 1H, C$\underline{H}$-6′-ppd), 2.63–2.48 (m, 3H, C$\underline{H}_2$Bn, C$\underline{H}$-1- ppd), 2.03 (d, J = 3.6 Hz, 2H, C$\underline{H}$-3- ppd; C$\underline{H}$-5- ppd), 1.84–1.66 (m, 5H, C$\underline{H}$-3′- ppd, C$\underline{H}$-4-ppd, C$\underline{H}$-5′-ppd, C$\underline{H}$-2-cyhex, C$\underline{H}$-6-cyhex), 1.63 (dd, J = 6.9, 4.1 Hz, 2H; C$\underline{H}_2$Bn), 1.42–1.10 (m, 8H; C$\underline{H}$-2′-cyhex, C$\underline{H}_2$-3-cyhex, C$\underline{H}_2$-4-cyhex, C$\underline{H}_2$-5-cyhex, C$\underline{H}$-6′-cyhex).

4.1.6.3. 1-(4-Benzylpiperazin-1-yl)-2-(phenylsulfanyl)ethan-1-one (24a). Yellow pale liquid, 260 mg (38% yield). ^{1}H NMR (400 MHz, $CDCl_3$) δ 6.97–6.90 (m, 2H, C$\underline{H}_{Ar}$-3,5), 6.87–6.68 (m, 8H, C$\underline{H}_{Thioph}$-2,3,4,5,6, C$\underline{H}_{Ar}$-2,4,6), 3.24 (s, 2H, SC$\underline{H}_2$CON), 3.12 (dd, J = 9.2, 4.1 Hz, 2H, C$\underline{H}$-2-ppz, C$\underline{H}$-6-ppz), 3.01 (s, 2H, C$\underline{H}_2$Bn), 3.00–2.95 (m, 2H, C$\underline{H}$-2′-ppz, C$\underline{H}$-6′-ppz), 1.92 (td, J = 8.5, 5.2 Hz, 4H, C$\underline{H}_2$-3-ppz, C$\underline{H}_2$-5-ppz). ^{13}C NMR (100 MHz, $CDCl_3$) δ 166.42 (CON), 136.94 (C$\underline{C}_{Ar}$-1), 134.31 (C$\underline{C}_{Thioph}$-1), 129.66 (C$\underline{H}_{Thioph}$-2,6), 128.39 (C$\underline{H}_{Thioph}$-3,5), 128.35 (C$\underline{H}_{Ar}$-3,5), 127.63 (C$\underline{H}_{Ar}$-2,6), 126.57 (C$\underline{H}_{Thioph}$-4), 126.30 (C$\underline{H}_{Ar}$-4), 61.72 (S$\underline{C}H_2$), 51.82 (C$\underline{H}_2$-2-ppz), 51.48 (C$\underline{H}_2$-6-ppz), 45.25 (C$\underline{H}_2$Bn), 40.80 (C$\underline{H}_2$-3-ppz), 35.42 (C$\underline{H}_2$-5-ppz).

4.1.6.4. 1-(4-Benzylpiperidin-1-yl)-2-(phenylsulfanyl)ethan-1-one (24b). Yellow pale liquid, 570 mg (83% yield). ^{1}H NMR (400 MHz, $CDCl_3$) δ 7.46 (d, J = 7.5 Hz, 2H, C$\underline{H}_{Ar}$-3,5), 7.35–7.27 (m, 4H, C$\underline{H}_{Thioph}$-2, 3, 5, 6), 7.24 (dt, J = 13.0, 6.4 Hz, 2H, C$\underline{H}_{Ar}$-2,6), 7.15 (d, J = 7.1 Hz, 2H, C$\underline{H}_{Ar}$-4, C$\underline{H}_{Thioph}$-4), 4.58 (d, J = 12.7 Hz, 1H, C$\underline{H}$-2-ppd), 3.83 (d, J = 13.3 Hz, 1H, C$\underline{H}$-2′-ppd), 3.77 (d, J = 1.6 Hz, 2H, SC$\underline{H}_2$CON), 3.00 (t, J = 12.6 Hz, 1H, C$\underline{H}$-6-ppd), 2.55 (dd, J = 16.9, 10.2 Hz, 3H, C$\underline{H}_2$Bn, C$\underline{H}$-6′-ppd), 1.83–1.64 (m, 3H, C$\underline{H}$-3-ppd, C$\underline{H}$-4-ppd, C$\underline{H}$-5-ppd), 1.33–1.09 (m, 2H, C$\underline{H}$-3′-ppd, C$\underline{H}$-5′-ppd). ^{13}C NMR (101 MHz, $CDCl_3$) δ 166.77 (CON), 139.88 (C$\underline{C}_{Ar}$-1), 135.27 (C$\underline{C}_{Thioph}$-1), 130.20 (C$\underline{H}_{Thioph}$-2,6), 129.09 (C$\underline{H}_{Thioph}$-3,5), 129.04 (C$\underline{H}_{Ar}$-3,5), 128.32 (C$\underline{H}_{Ar}$-2,6), 126.89 (C$\underline{H}_{Thioph}$-4), 126.09 (C$\underline{H}_{Ar}$-4), 46.81 (C$\underline{H}_2$-2-ppd) 42.91 (C$\underline{H}_2$Bn), 42.46 (C$\underline{H}_2$-6-ppd), 38.08 (SC$\underline{H}_2$CO), 36.89 (C$\underline{H}_2$-4-ppd), 32.48 (C$\underline{H}_2$-3-ppd), 31.73 (C$\underline{H}_2$-5-ppd).

4.1.7. General procedure for the synthesis of amines 3a-b, 7a-b

To a solution of $LiAlH_4$ (1.5 eq.) in THF dry (5 mL), at 0 °C under argon atmosphere amide derivate 14a-b, 24a-b (1 eq.) was added, and the suspension was stirred in the same condition for 1 h and then at room temperature overnight. The mixture was carefully quenched with water and filtered through a Celite pad. The filtrate was basified with 1 N aqueous NaOH and extracted with AcOEt. The organic layer was washed with brine, dried over anhydrous Na_2SO_4 and concentrated.

4.1.7.1. 1-Benzyl-4-[2-(cyclohexylsulfanyl)ethyl]piperazine (3a). The product was purified by silica gel column chromatography (crude:silica gel 1:100; CE:AcOEt 7:3) to give 46 mg of a yellow oil, (10% yield). ^{1}H NMR (400 MHz, $CDCl_3$) δ 7.24 (d, J = 4.4 Hz, 4H, C$\underline{H}_{Ar}$-2,3,5,6), 7.21–7.14 (m, 1H, C$\underline{H}_{Ar}$-4), 3.44 (s, 2H, C$\underline{H}_2$Bn), 2.64–2.54 (m, 2H, CyhexSC$\underline{H}_2$), 2.54–2.47 (m, 2H, SCH$_2$C$\underline{H}_2$N), 2.43 (s, 6H, C$\underline{H}$-2-ppz, C$\underline{H}$-2′-ppz, C$\underline{H}$-3-ppz, C$\underline{H}$-5-ppz, C$\underline{H}$-6-ppz, C$\underline{H}$-6′-ppz), 1.94–1.81 (m, 2H, C$\underline{H}$-3′-ppz, C$\underline{H}$-5′-ppz), 1.69 (d, J = 3.5 Hz, 3H, C$\underline{H}$-2-cyhex, C$\underline{H}$-4-cyhex, C$\underline{H}$-6-cyhex), 1.54 (d, J = 8.7 Hz, 1H, C$\underline{H}$-1-cyhex), 1.31–1.08 (m, 7H, C$\underline{H}$-2′-cyhex, C$\underline{H}_2$-3-cyhex, C$\underline{H}$-4′-cyhex, C$\underline{H}_2$-5-cyhex, C$\underline{H}$-6′-cyhex). ^{13}C NMR (101 MHz, $CDCl_3$) δ 138.06 (C$\underline{C}_{Ar}$-1), 129.22 (C$\underline{H}_{Ar}$-3,5), 128.20 (C$\underline{H}_{Ar}$-2,6), 127.04 (C$\underline{H}_{Ar}$-4), 63.04 (C$\underline{H}_2$Bn), 58.96 (C$\underline{H}_2$-2-ppz, C$\underline{H}_2$-6-ppz), 53.11 (C$\underline{H}_2$-3-ppz, C$\underline{H}_2$-5-ppz), 52.96 (SCH$_2$C$\underline{H}_2$N), 43.77 (C$\underline{H}$-1-cyhex), 33.79 (C$\underline{H}_2$-2-cyhex, C$\underline{H}_2$-6-cyhex), 27.15 (SC$\underline{H}_2$CH$_2$N), 26.13 (C$\underline{H}_2$-4-cyhex), 25.82 (C$\underline{H}_2$-3-cyhex, C$\underline{H}_2$-5-cyhex).

4.1.7.2. 4-Benzyl-1-[2- (cyclohexylsulfanyl)ethyl]piperidine (3b). The product was purified by silica gel column chromatography (crude:silica gel: 1:100; CE:AcOEt 6:4) to give 130 mg of a yellow oil (50% yield). ^{1}H NMR (400 MHz, $CDCl_3$) δ 7.19 (dd, J = 8.4, 6.3 Hz, 2H, C$\underline{H}_{Ar}$-3,5), 7.13–7.08 (m, 1H, C$\underline{H}_{Ar}$-4), 7.08–7.04 (m, 2H, C$\underline{H}_{Ar}$-2,6), 2.83 (d, J = 11.6 Hz, 2H, C$\underline{H}_2$N), 2.63–2.52 (m, 2H, CyhexSC$\underline{H}_2$), 2.49–2.41 (m, 4H, C$\underline{H}_2$Bn, C$\underline{H}$-2-ppd, C$\underline{H}$-6-ppd), 1.86 (ddd, J = 23.2, 10.6, 3.2 Hz, 4H, C$\underline{H}$-2′-ppd, C$\underline{H}$-3-ppd, C$\underline{H}$-5-ppd, C$\underline{H}$-6′-ppd), 1.77 (s, 2H, C$\underline{H}$-3′-ppd, C$\underline{H}$-5′-ppd), 1.69 (d, J = 3.5 Hz, 2H, C$\underline{H}$-2-cyhex, C$\underline{H}$-6-cyhex), 1.56 (d, J = 12.9 Hz, 3H, C$\underline{H}$-1-cyhex, C$\underline{H}$-2′-cyhex, C$\underline{H}$-6′-cyhex), 1.44 (dqd, J = 14.6, 7.2, 3.5 Hz, 1H, C$\underline{H}$-4-ppd), 1.31–1.09 (m, 6H, C$\underline{H}_2$-3-cyhex, C$\underline{H}_2$-4-cyhex, C$\underline{H}_2$-5-cyhex). ^{13}C NMR (101 MHz, $CDCl_3$) δ 140.65 (C$\underline{C}_{Ar}$-1), 129.12 (C$\underline{H}_{Ar}$-3,5), 128.16 (C$\underline{H}_{Ar}$-2,6), 125.78 (C$\underline{H}_{Ar}$-4), 59.33 (C$\underline{H}_2$-2-ppd, C$\underline{H}_2$-6-ppd), 53.89 (C$\underline{H}_2$N), 43.74 (C$\underline{H}$-1-cyhex), 43.18 (C$\underline{H}_2$Bn), 37.87 (C$\underline{H}$-4-ppd), 33.80 (C$\underline{H}_2$-3-ppd, C$\underline{H}_2$-5-ppd), 32.09 (C$\underline{H}_2$-2-cyhex, C$\underline{H}_2$-6-cyhex), 27.31 (CyhexSC$\underline{H}_2$), 26.14 (C$\underline{H}_2$-4-cyhex), 25.82 (C$\underline{H}_2$-3-cyhex, C$\underline{H}_2$-5-cyhex).

4.1.7.3. 1-Benzyl-4-[2-(phenylsulfanyl)ethyl]piperazine (7a). The product was purified by silica gel column chromatography (crude:silica gel: 1:100; CE:AcOEt 6:4) to give 56 mg of a yellow oil (23% yield). ^{1}H NMR (400 MHz, $CDCl_3$) δ 6.86–6.73 (m, 9H, C$\underline{H}_{Ar}$-2,3,4,5,6, C$\underline{H}_{Thioph}$-2,3,5,6), 6.69–6.63 (m, 1H, C$\underline{H}_{Thioph}$-4), 3.01 (s, 2H, C$\underline{H}_2$Bn), 2.63–2.50 (m, 2H, SC$\underline{H}_2$), 2.19–2.10 (m, 2H, CH$_2$N), 2.00 (s, 8H, C$\underline{H}_2$-2-ppz, C$\underline{H}_2$-3-ppz, C$\underline{H}_2$-5-ppz, C$\underline{H}_2$-6-ppz).

4.1.7.4. 4-Benzyl-1-[2-(phenylsulfanyl)ethyl]piperidine (7b). Yellow pale liquid, 480 mg (88% yield). ^{1}H NMR (400 MHz, $CDCl_3$) δ 7.36 (dd, J = 8.2, 1.0 Hz, 2H, CH_{Ar}-3,5), 7.29 (dd, J = 8.7, 4.9 Hz, 4H, CH_{Thioph}-2,3,5,6), 7.18 (dt, J = 8.3, 7.3 Hz, 4H, CH_{Ar}-2,4,6, CH_{Thioph}-4), 3.17–3.01 (m, 2H, ArSCH_2), 2.94 (d, J = 11.4 Hz, 2H, CH-2-ppd, CH-6-ppd), 2.71–2.60 (m, 2H, CH_2N), 2.56 (d, J = 7.1 Hz, 2H, CH_2Bn), 1.98 (t, J = 10.8 Hz, 2H, CH-2′-ppd, CH-6′-ppd), 1.66 (d, J = 13.0 Hz, 2H, CH-3-ppd, CH-5-ppd), 1.54 (dtd, J = 14.6, 7.4, 3.7 Hz, 1H, CH-4-ppd), 1.44–1.19 (m, 2H, CH-3′-ppd, CH-5′-ppd). ^{13}C NMR (101 MHz, $CDCl_3$) δ 140.60 (C$_{Ar}$-1), 136.41 (C$_{Thioph}$-1), 129.12 (CH_{Thioph}-2,6), 128.96 (CH_{Thioph}-3,5), 128.90 (CH_{Ar}-3,5), 128.18 (CH_{Ar}-2,6), 125.88 (CH_{Thioph}-4), 125.82 (CH_{Ar}-4), 58.05 (CH_2-2-ppd,CH_2-6-ppd), 53.85 (CH_2N), 43.15 (CH_2Bn), 37.81 (CH_2-4-ppd), 32.02 (SCH_2), 30.76 (CH_2-3-ppd, CH_2-5-ppd).

4.1.8. General procedure for the synthesis of bromopropyl derivates 9, 18 and 25

To a solution of alcohol derivate (1eq.) in acetone or DMF (10 mL), K_2CO_3 (2.5 eq) and 1,3-dibromopropane (2–3 eq.) were added and the reaction mixture was stirred at room temperature for 4–24 h. The suspension was filtered and concentrated. The residue was suspended in diethyl ether and the organic phase was washed with 1 N aqueous NaOH, brine, dried over anhydrous Na_2SO_4 and concentrated.

4.1.8.1. [(3-bromopropyl)sulfanyl]cyclohexane (9). The product was purified by silica gel column chromatography (crude:silica gel: 1:100; CE 100%) to give 974 mg of a colorless oil, (48% yield). ^{1}H NMR (400 MHz, $CDCl_3$) δ 3.52 (t, J = 6.5 Hz, 2H, CH_2Br), 2.68 (t, J = 7.0 Hz, 2H, CyhexSCH_2), 2.65–2.60 (m, 1H, CH-1-cyhex), 2.10 (p, J = 6.7 Hz, 2H, SCH$_2$CH_2CH$_2$Br), 2.01–1.89 (m, 2H, CH-2-cyhex, CH-6-cyhex), 1.77 (d, J = 2.5 Hz, 2H, CH-3-cyhex, CH-5-cyhex), 1.62 (dd, J = 9.3, 1.6 Hz, 1H; CH-4-cyhex), 1.39–1.17 (m, 5H, CH-2′-cyhex, CH-3′-cyhex, CH-4′-cyhex, CH-5′-cyhex, CH-6′-cyhex). ^{13}C NMR (101 MHz, CDCl3) δ 43.60 (CH-1-cyhex), 33.71 (CyhexSCH_2), 32.78 (CH_2-2-cyhex, CH_2-6-cyhex), 32.44 (SCH$_2$CH_2CH$_2$Br), 28.25 (CH_2Br), 26.10 (CH_2-4-cyhex), 25.82 (CH_2-3-cyhex, CH_2-5-cyhex).

4.1.8.2. [(3-bromopropyl)sulfanyl]benzene (18). The product was purified by silica gel column chromatography (crude:silica gel: 1:100; CE 100%) to give 265 mg of a colorless oil (33% yield). ^{1}H NMR (400 MHz, $CDCl_3$) δ 7.41–7.36 (m, 2H, CH_{Ar}-2,6), 7.35–7.27 (m, 2H, CH_{Ar}-3,5), 7.23 (ddd, J = 7.2, 3.9, 1.3 Hz, 1H, CH_{Ar}-4), 3.55 (t, J = 6.4 Hz, 2H, CH_2Br), 3.10 (t, J = 6.9 Hz, 2H, SCH_2CH$_2$CH$_2$Br), 2.23–2.12 (m, 2H, SCH$_2$CH_2CH$_2$Br). ^{13}C NMR (101 MHz, $CDCl_3$) δ 135.61 (C$_{Ar}$-1), 129.64 (CH_{Ar}-2,6), 129.02 (CH_{Ar}-3,5), 126.32 (CH_{Ar}-4), 32.01 (SCH_2CH$_2$CH$_2$Br), 31.97 (CH_2Br), 31.77 (SCH$_2$CH_2CH$_2$Br).

4.1.8.3. (3-bromopropoxy)benzene) (25). Yellow oil, 1.68g (73% yield). ^{1}H NMR (400 MHz, $CDCl_3$) δ 7.27 (dd, J = 6.6, 8.5 Hz, 2H, CH_{Ar}-3,5), 7.06–6.82 (m, 3H, CH_{Ar}-2,4,6), 4.08 (t, J = 4.9 Hz, 2H, CH_2O), 3.50 (t, J = 7.9 Hz, 2H, CH_2Br), 2.13 (tt, J = 4.8, 7.9 Hz, 2H, OCH$_2$CH_2CH$_2$Br).

4.1.9. Synthesis of 1,5-dioxaspiro[5.5]undecane (15)

To a solution of cyclohexanone (2.11 mL, 20.4 mmol, 1eq.) in dry toluene at room temperature and under nitrogen atmosphere, propane-1,3-diol (2.21 mL, 33 mmol, 1.5 eq.) and pTSA (351 mg, 2.04 mmol, 0.1 eq.). The mixture was refluxed using a Dean-Stark apparatus to trap the forming water for 2 h. Thereafter, the reaction was chilled at room temperature and diluted with Et_2O. The organic phase was washed with a saturated solution of Na_2CO_3, dried over anhydrous Na_2SO_4 and concentrated to give 2.0 g of a yellow liquid which was purified by silica gel column chromatography (crude:silica gel 1:75; CE:AcOEt 9:1) to give 1.12 g of a colorless liquid (35% yield). ^{1}H NMR (400 MHz, $CDCl_3$) δ 3.92 (t, J = 5.5 Hz, 4H, COCH_2, COCH_2), 1.82–1.67 (m, 6H, CH_2-3-cyhex, CH_2-5-cyhex, OCH$_2$CH_2CH$_2$O), 1.54 (dt, J = 11.5, 6.0 Hz, 4H, CH_2-2-cyhex, CH_2-6-cyhex), 1.42 (s, 2H, CH_2-4-cyhex).

4.1.10. Synthesis of 3-(cyclohexyloxy)propan-1-ol (16)

To a solution of anhydrous $AlCl_3$ (648 mg, 4.86 mmol, 2 eq.) in dry Et_2O at 0 °C and under nitrogen atmosphere, 2 M $LiAlH_4$ in diethyl ether (607 μL, 1.22 mmol, 0.5 eq.) was added and the suspension was stirred in the same conditions for 15 min 23 (BS444) (380 mg, 2.43 mmol, 1 eq.), solubilized in 5 mL of dry diethyl ether, was added to the first suspension, and stirred at room temperature for 2 h. The reaction was chilled in an ice bath and carefully quenched with 787 μL of water (43.7 mmol, 18 eq.) followed by the same volume of 3 M aqueous KOH, and 2 mL of water, and in the same condition for an additional hour. The aqueous phase was extracted with Et_2O, and the organic phase dried over anhydrous Na_2SO_4 and concentrated to give 350 mg (91% yield) of a colorless liquid, which was pure enough to be used in the next step without further purification. ^{1}H NMR (400 MHz, $CDCl_3$) δ 3.78 (dd, J = 11.9, 6.5 Hz, 2H, OCH$_2$CH$_2$CH_2OH), 3.67 (t, J = 5.7 Hz, 2H, CyhexOCH_2), 3.28 (s, 1H, CH-1-cyhex), 1.98–1.64 (m, 6H, OCH$_2$CH_2CH$_2$OH, CH-2-cyhex, CH-3-cyhex, CH-5-cyhex, CH-6-cyhex), 1.53 (d, J = 5.9 Hz, 1H, CH-4-cyhex), 1.41–1.15 (m, 5H, CH-2′-cyhex, CH-3′-cyhex, CH-4′-cyhex CH-5′-cyhex, CH-6′-cyhex). ^{13}C NMR (101 MHz, $CDCl_3$) δ 77.84 (CH-1-cyhex), 67.65 (CyhexOCH_2), 62.75 (OCH$_2$CH$_2$CH_2OH), 32.13 (OCH$_2$CH_2CH$_2$OH), 32.05 (CH_2-2-cyhex, CH_2-6-cyhex), 25.75 (CH_2-4-cyhex), 23.91 (CH_2-3-cyhex, CH_2-5-cyhex).

4.1.11. Synthesis of (2-chloroethoxy)cyclohexane (11)

2-(cyclohexyloxy)ethan-1-ol (500 μL, 3.44 mmol, 1 eq.) was solubilized in 5 mL of $SOCl_2$ and a drop of DMF, as catalyst was added. The solution was refluxed for 5 h and concentrated under reduced pressure. The residue was triturated with crushed ice and diluted with water. Solid $NaHCO_3$ was added until neutralization and the aqueous phase was extracted with Et_2O. The organic layer was dried over anhydrous Na_2SO_4 and concentrated to give 320 mg (57% yield) of an orange liquid, which was pure enough to be used in the next step without further purification.

^{1}H NMR (400 MHz, $CDCl_3$) δ 3.73 (t, J = 6.0 Hz, 2H, CyhexOCH_2), 3.62 (dd, J = 9.2, 3.1 Hz, 2H, CH_2Cl), 3.36–3.25 (m, 1H, CH-1-cyhex), 2.00–1.85 (m, 2H, CH-2-cyhex, CH-6-cyhex), 1.77 (dd, J = 9.1, 4.4 Hz, 2H, CH-3-cyhex, CH-5-cyhex), 1.56 (dd, J = 15.9, 9.7 Hz, 1H, CH-4-cyhex), 1.40–1.14 (m, 5H, CH-2′-cyhex, CH-3′-cyhex, CH-4′-cyhex, CH-5′-cyhex, CH-6′-cyhex). ^{13}C NMR (101 MHz, $CDCl_3$) δ 78.19 (CH-1-cyhex), 68.08 (CyhexOCH_2), 43.25 (CH_2Cl), 32.20 (CH_2-2-cyhex, CH_2-6-cyhex), 25.72 (CH_2-4-cyhex), 24.07 (CH_2-3-cyhex, CH_2-5-cyhex).

4.1.12. Synthesis of (3-chloropropoxy)cyclohexane (17)

16 (350 mg, 2.21 mmol, 1 eq.) was solubilized in 5 mL of $SOCl_2$ and a drop of DMF, as catalyst was added. The solution was refluxed for 2 h and concentrated under reduced pressure. The residue was triturated with crushed ice and diluted with water. Solid $NaHCO_3$ was added until neutralization and the aqueous phase was extracted with Et_2O. The organic layer was dried over anhydrous Na_2SO_4 and concentrated to give 300 mg (77% yield) of a yellow liquid, which was pure enough to be used in the next step without further purification.

^{1}H NMR (400 MHz, $CDCl_3$) δ 3.59 (t, J = 6.4 Hz, 2H, CH_2Cl) 3.51 (t, J = 5.9 Hz, 2H, -OCH_2), 3.16 (dt, J = 8.7, 3.9 Hz, 1H, CH-1-cyhex), 1.93 (p, J = 6.1 Hz, 2H, OCH$_2$CH_2CH$_2$Cl), 1.89–1.74 (m, 2H, CH-2-cyhex, CH-6-cyhex), 1.66 (d, J = 4.3 Hz, 2H, CH-3-cyhex, CH-5-cyhex), 1.49 (dd, J = 21.5, 7.4 Hz, 1H, CH-4-cyhex), 1.30–1.05 (m, 5H, CH-2′-cyhex, CH-3′-cyhex, CH-4′-cyhex, CH-5′-cyhex, CH-6′-cyhex). ^{13}C NMR (101 MHz, $CDCl_3$) δ 77.64 (CH-1-cyhex), 64.04 (CyhexOCH_2), 42.22 (CH_2Cl), 33.17 (CH_2-2-cyhex, CH_2-6-cyhex), 32.23 (OCH$_2$CH_2CH$_2$Cl), 25.82 (CH_2-4-cyhex), 24.09 (CH_2-3-cyhex, CH_2-5-cyhex).

4.1.13. General procedure for the synthesis of amines 1a-b, 2a-b, 4a-b, 5a-b, 6a-b, 8a-b

To a solution of 4-benzylpiperidine or 1-benzylpiperidine (1.2 eq) in

DMSO, K_2CO_3 (2.5 eq.) was added, and the suspension was stirred at room temperature for 10 min. Thereafter, a solution of the appropriate halogen derivative in DMSO (5 mL) was added and the mixture stirred at room temperature for 3–76 h. The mixture was diluted with AcOEt, and the organic layer was washed sequentially with water and brine, dried over anhydrous Na_2SO_4 and concentrated. The product was purified by silica gel to give the title compound.

4.1.13.1. 1-Benzyl-4-[3-(cyclohexylsulfanyl)propyl]piperazine (1a). The product was purified on silica gel column chromatography (crude/silica gel: 1:100; DCM: MeOH 95:5). Colorless liquid, 234 mg (56% yield). ^{1}H NMR (400 MHz, $CDCl_3$) δ 7.38–7.23 (m, 5H, CH_{Ar}-2,3,4,5,6), 3.53 (s, 2H,CH_2Bn), 2.65 (td, J = 10.4, 4.9 Hz, 1H, CH-1-cyhex), 2.60–2.38 (m, 10H, CyhexSCH_2, CH_2-2-ppz, CH_2-3-ppz, CH_2-5-ppz, CH_2-6-ppz), 2.04–1.92 (m, 2H, CH_2N), 1.88–1.70 (m, 4H, SCH$_2$CH_2CH$_2$N, CH-2-cyhex, CH-6-cyhex), 1.63 (d, J = 7.1 Hz, 1H, CH-4-cyhex), 1.40–1.20 (m, 7H, CH-2′-cyhex, CH-4′-cyhex, CH-6′-cyhex, CH_2-3-cyhex, CH_2-5-cyhex). ^{13}C NMR (101 MHz, $CDCl_3$) δ 138.14 (C$_{Ar}$-1), 129.22 (CH_{Ar}-3,5), 128.19 (CH_{Ar}-2,6), 127.01 (CH_{Ar}-4), 63.09 (CH_2N), 57.66 (CH_2-2-ppz, CH_2-6-ppz), 53.24 (CH-1-cyhex), 53.09 (CH_2Bn), 43.46 (CH_2-2-cyhex, CH_2-6-cyhex), 33.72 (s, SCH$_2$CH$_2$CH$_2$N), 28.06 (CH_2-3-ppz, CH_2-5-ppz), 27.42 (CyhexSCH_2), 26.15 (CH_2-4-cyhex), 25.87 (CH_2-3-cyhex, CH_2-5-cyhex).

4.1.13.2. 4-Benzyl-1-[3-(cyclohexylsulfanyl)propyl]piperidine (1b). The product was purified on silica gel column chromatography (crude:silica gel: 1:60; DCM:MeOH 95:5). Yellow liquid, 339 mg (81% yield). ^{1}H NMR (400 MHz, $CDCl_3$) δ 7.29 (dd, J = 8.9, 5.8 Hz, 2H, CH_{Ar}-3,5), 7.21 (d, J = 7.3 Hz, 1H, CH_{Ar}-4), 7.16 (t, J = 7.0 Hz, 2H, CH_{Ar}-2,6), 2.92 (d, J = 11.5 Hz, 2H, CH-2-ppd, CH-6-ppd), 2.65 (td, J = 10.3, 5.0 Hz, 1H, CH-1-cyhex), 2.56 (t, J = 6.5 Hz, 4H, CH-3-ppd, CH-5-ppd, CH_2Bn), 2.44–2.38 (m, 2H, CH_2N), 2.02–1.95 (m, 2H, CH-2-cyhex, CH-6-cyhex), 1.90 (t, J = 11.7 Hz, 2H, CH-2′-ppd, CH-6′-ppd), 1.79 (dt, J = 14.6, 7.4 Hz, 4H, CyhexSCH_2, CH-3′-ppd, CH-5′-ppd), 1.65 (d, J = 12.6 Hz, 3H, SCH$_2$CH_2CH$_2$N, CH-4-cyhex), 1.54 (dddd, J = 14.6, 11.0, 7.2, 3.5 Hz, 1H, CH-4-ppd), 1.42–1.18 (m, 7H, CH-2′-cyhex, CH_2-3-cyhex, CH-4′-cyhex, CH_2-5-cyhex, CH-6′-cyhex). ^{13}C NMR (101 MHz, $CDCl_3$) δ 140.70 (C$_{Ar}$-1), 129.12 (CH_{Ar}-3,5), 128.16 (CH_{Ar}-2,6), 125.78 (CH_{Ar}-4), 58.05 (CH_2N), 53.97 (CH_2-2-ppd, CH_2-6-ppd), 43.45 (CH-1-cyhex), 43.20 (CH_2Bn), 37.93 (CH-4-ppd), 33.71 (CH_2-2-cyhex, CH_2-6-cyhex), 32.11 (SCH$_2$CH_2CH$_2$N), 28.17 (CH_2-3-ppd, CH_2-5-ppd), 27.49 (CyhexSCH_2), 26.15 (CH_2-4-cyhex), 25.87 (CH_2-3-cyhex, CH_2-5-cyhex).

4.1.13.3. 1-Benzyl-4-[2-(cyclohexyloxy)ethyl]piperazine (2a). The product was purified on silica gel column chromatography (crude:silica gel 1:100; DCM:MeOH 95:5). Orange liquid, 90 mg (19% yield). ^{1}H NMR (400 MHz, $CDCl_3$) δ 7.32 (t, J = 6.5 Hz, 4H, CH_{Ar}-2,3,5,6), 7.28–7.23 (m, 1H, CH_{Ar}-4), 3.61 (t, J = 6.3 Hz, 2H, CH_2Bn), 3.53 (s, 2H, CyhexOCH_2), 3.23 (td, J = 8.9, 4.0 Hz, 1H, CH-1-cyhex), 2.64–2.42 (m, 10H, CH_2N, CH_2-2-ppz, CH_2-3-ppz, CH_2-5-ppz, CH_2-6-ppz), 1.95–1.67 (m, 4H, CH-2-cyhex, CH-3-cyhex, CH-5-cyhex, CH-6-cyhex), 1.54 (d, J = 6.7 Hz, 1H, CH-4-cyhex), 1.34–1.14 (m, CH-2′-cyhex, CH-3′-cyhex, CH-4′-cyhex, CH-5′-cyhex, CH-6′-cyhex). ^{13}C NMR (101 MHz, $CDCl_3$) δ 138.12 (C$_{Ar}$-1), 129.23 (CH_{Ar}-3,5), 128.18 (CH_{Ar}-2,6), 127.01 (CH_{Ar}-4), 77.86 (CH-1-cyhex), 65.63 (CyhexOCH_2), 63.08 (CH_2Bn), 58.20 (CH_2N), 53.67 (CH_2-2-ppz, CH_2-6-ppz), 53.02 (CH_2-3-ppz, CH_2-5-ppz), 32.25 (CH_2-2-cyhex, CH_2-6-cyhex), 25.82 (CH_2-4-cyhex), 24.19 (CH_2-3-cyhex, CH_2-5-cyhex).

4.1.13.4. 4-Benzyl-1-[2-(cyclohexyloxy)ethyl]piperidine (2b). The product was purified on silica gel column chromatography (crude:silica gel 1:100; DCM:MeOH 9:1). Colorless liquid, 127 mg (45% yield). ^{1}H NMR (400 MHz, $CDCl_3$) δ 7.29 (dd, J = 8.4, 6.5 Hz, 2H, CH_{Ar}-3,5), 7.24–7.12 (m, 3H, CH_{Ar}-2,4,6), 3.61 (t, J = 6.4 Hz, 2H, CyhexOCH_2), 3.28–3.18 (m, 1H, CH-1-cyhex), 2.96 (d, J = 11.4 Hz, 2H, CH-2-ppd, CH-6-ppd), 2.59 (t, J = 6.4 Hz, 2H,CH_2N), 2.55 (d, J = 7.0 Hz, 2H, CH_2Bn), 2.02 (t, J = 11.4 Hz, 2H, CH-2′-ppd, CH-6′-ppd), 1.96–1.84 (m, 2H, CH-2-cyhex, CH-6-cyhex), 1.74 (d, J = 4.3 Hz, 2H, CH-3-ppd, CH-5-ppd), 1.64 (d, J = 12.8 Hz, 2H, CH-3-cyhex, CH-5-cyhex), 1.59–1.48 (m, 2H, CH-4-cyhex, CH-4-ppd), 1.42–1.15 (m, 7H, CH-3′-ppd, CH-5′-ppd, CH-2′-cyhex, CH-3′-cyhex, CH-4′-cyhex, CH-5′-cyhex, CH-6′-cyhex).

^{13}C NMR (101 MHz, $CDCl_3$) δ 140.69 (CH_{Ar}-1), 129.12 (CH_{Ar}-3,5), 128.15 (CH_{Ar}-2,6), 125.77 (CH_{Ar}-4), 77.85 (CH-1-cyhex), 65.68 (CyhexOCH_2), 58.47 (CH_2N), 54.38 (CH_2-2-ppd, CH_2-6-ppd), 43.18 (CH_2Bn), 37.73 (CH-4-ppd), 32.26 (CH_2-2-cyhex, CH_2-6-cyhex), 32.05 (CH_2-3-ppd, CH_2-5-ppd), 25.82 (CH_2-4-cyhex), 24.19 (CH_2-3-cyhex, CH_2-5-cyhex).

4.1.13.5. 1-Benzyl-4-[3-(cyclohexyloxy)propyl]piperazine (4a). The product was purified on silica gel column chromatography (crude:silica gel 1:70; DCM:MeOH 95:5). Yellow oil, 200 mg (56% yield). ^{1}H NMR (400 MHz, $CDCl_3$) δ 7.39–7.17 (m, 5H, CH_{Ar}-2,3,4,5,6), 3.57–3.46 (m, 4H, CyhexOCH_2, CH_2Bn), 3.26–3.16 (m, 1H, CH-1-cyhex), 2.46 (dd, J = 20.8, 13.4 Hz, 10H, CH_2-2-ppz, CH_2-3-ppz, CH_2-5-ppz, CH_2-6-ppz, CH_2N), 1.91 (d, J = 10.1 Hz, 2H; CH-2-cyhex, CH-6-cyhex), 1.76 (dt, J = 13.3, 6.5 Hz, 4H, CH-3-cyhex, CH-5-cyhex, OCH$_2$CH_2CH$_2$N), 1.54 (d, J = 5.7 Hz, 1H, CH-4-cyhex), 1.36–1.12 (m, 5H, CH-2′-cyhex, CH-3′-cyhex, CH-4′-cyhex, CH-5′-cyhex, CH-6′-cyhex). ^{13}C NMR (101 MHz, $CDCl_3$) δ 138.15 (C$_{Ar}$-1), 129.24 (CH_{Ar}-3,5), 128.19 (CH_{Ar}-2,6), 127.00 (CH_{Ar}-4), 77.42 (CH-1-cyhex), 66.19 (CyhexOCH_2), 63.09 (CH_2Bn), 55.65 (CH_2-2-ppz, CH_2-6-ppz), 53.23 (CH_2-3-ppz, CH_2-5-ppz), 53.08 (CH_2N), 32.32 (CH_2-2-cyhex, CH_2-6-cyhex), 27.62 (OCH$_2$CH_2CH$_2$N), 25.86 (CH_2-4-cyhex), 24.21 (CH_2-3-cyhex, CH_2-5-cyhex).

4.1.13.6. 4-Benzyl-1-[3-(cyclohexyloxy)propyl]piperidine (4b). The product was purified on silica gel column chromatography (crude:silica gel 1:50; DCM:MeOH 9:1). Yellow oil, 53 mg (30% yield). ^{1}H NMR (400 MHz, $CDCl_3$) δ 7.29 (dd, J = 8.8, 6.2 Hz, 2H, CH_{Ar}-3,5), 7.25–7.10 (m, 3H, CH_{Ar}-2,4,6), 3.48 (q, J = 6.7 Hz, 2H, CyhexOCH_2), 3.30–3.13 (m, 1H, CH-1-cyhex), 2.92 (d, J = 11.4 Hz, 2H, CH-2-ppd, CH-6-ppd), 2.54 (t, J = 7.8 Hz, 2H, CH_2Bn), 2.47–2.35 (m, 2H, CH_2N), 1.89 (t, J = 10.6 Hz, 5H, CH-2′-ppd, CH-6′-ppd, CH-2-cyhex, CH-6-cyhex, CH-4-ppd), 1.83–1.70 (m, 4H, CH-3-ppd, CH-5-ppd, OCH$_2$CH_2CH$_2$N), 1.65 (d, J = 13.1 Hz, 2H, CH-3-cyhex, CH-5-cyhex), 1.53 (ddd, J = 14.6, 7.3, 3.4 Hz, 2H, CH-3′-ppd, CH-5′-ppd), 1.42–1.14 (m, 6H, CH-2′-cyhex, CH-3′-cyhex, CH_2-4-cyhex, CH-5′-cyhex, CH-6′-cyhex). ^{13}C NMR (101 MHz, $CDCl_3$) δ 140.76 (C$_{Ar}$-1), 129.12 (CH_{Ar}-3,5), 128.15 (CH_{Ar}-2,6), 125.75 (CH_{Ar}-4), 77.41 (CyhexOCH_2), 66.33 (CH-1-cyhex), 56.02 (CH_2-2-ppd, CH_2-6-ppd), 53.94 (CH_2N), 43.22 (CH_2Bn), 37.96 (CH-4-ppd), 32.33 (CH_2-2-cyhex, CH_2-6-cyhex), 32.15 (CH_2-3-ppd, CH_2-5-ppd), 27.72 (OCH$_2$CH_2CH$_2$N), 25.86 (CH_2-4-cyhex), 24.22 (CH_2-3-cyhex, CH_2-5-cyhex).

4.1.13.7. 1-Benzyl-4-[3-(phenylsulfanyl)propyl]piperazine (5a). The product was purified by column chromatography (crude: silica gel 1:150; CE:AcOEt 1:1). Yellow pale oil, 159 mg (56% yield). ^{1}H NMR (400 MHz, $CDCl_3$) δ 7.18 (t, J = 5.9 Hz, 6H, CH_{Ar}-2,3,5,6, CH_{Thioph}-2,6), 7.12 (dd, J = 8.8, 6.4 Hz, 3H, CH_{Thioph}-3,4,5), 7.02 (t, J = 7.2 Hz, 1H CH_{Ar}-4), 3.38 (s, 2H, CH_2Bn), 2.81 (t, J = 7.2 Hz, 2H,CH_2N), 2.35 (s, 10H, CyhexSCH_2, CH_2-2-ppz, CH_2-3-ppz, CH_2-5-ppz, CH_2-6-ppz), 1.77–1.62 (m, 2H, SCH$_2$CH_2CH$_2$N).

4.1.13.8. 4-Benzyl-1-[3-(phenylsulfanyl)propyl]piperidine (5b). The product was purified by column chromatography (crude: silica gel 1:100; DCM:MeOH 9:1). Yellow pale oil, 58 mg (63% yield). ^{1}H NMR (400 MHz, $CDCl_3$) δ 7.32 (ddd, J = 14.9, 8.1, 2.0 Hz, 6H,CH_{Ar}-3,5, CH_{Thioph}-2,3,5,6), 7.20 (dd, J = 13.3, 7.2 Hz, 2H, CH_{Ar}-2,6), 7.15 (d, J = 7.1 Hz, 2H, CH_{Ar}-4, CH_{Thioph}-4), 2.98 (t, J = 7.1 Hz, 4H, NCH_2, CH-2-pip, CH-6-pip), 2.56 (t, J = 7.9 Hz, 4H, CH_2Bn, CH-2′-pip, CH-6′-pip), 1.99 (d, J = 37.4 Hz, 4H, SCH_2, CH-2-pip, CH-6-pip), 1.77–1.40 (m, 5H,

$SCH_2CH_2CH_2N$, CH-3′-ppd, CH-4-ppd, CH-5′-ppd). ^{13}C NMR (101 MHz, $CDCl_3$) δ 140.18 (C_{Ar}-1), 136.04 (CH_{Thioph}-1), 129.36 (CH_{Thioph}-2,6), 129.07 (CH_{Thioph}-3,5), 128.97 (CH_{Ar}-3,5), 128.28 (CH_{Ar}-2,6), 126.14 (CH_{Thioph}-4), 125.98 (CH_{Ar}-4), 57.12 (CH_2N), 53.61 (CH_2-2-ppd, CH_2-6-ppd), 42.75 (CH_2Bn), 37.45 (CH_2-4-ppd), 31.61 (CH_2-3-ppd, CH_2-5-ppd), 30.98 (CyhexSCH_2), 29.70 ($SCH_2CH_2CH_2N$).

4.1.13.9. 1-Benzyl-4-(2-phenoxyethyl)piperazine (6a). The product was purified by column chromatography (crude: silica gel 1:150; CE:AcOEt 1:1). Colorless oil, 189 mg (66% yield). ^1H NMR (400 MHz, $CDCl_3$) δ 7.37–7.22 (m, 7H, CH_{Phen}-3,5, CH_{Bn}-2,3,4,5,6), 6.97–6.85 (m, 3H, CH_{Phen}-2,4,6), 4.11 (t, J = 6.3 Hz, 2H, CH_2OPh), 3.53 (s, 2H, CH_2Bn), 2.84 (t, J = 5.8 Hz, 2H, CH_2N), 2.59 (d, J = 43.6 Hz, 8H, CH_2-2-ppz, CH_2-3-ppz, CH_2-5-ppz, CH_2-6-ppz). ^{13}C NMR (101 MHz, $CDCl_3$) δ 158.69 (CH_{Phen}-1), 137.75 (C_{Bn}-1), 129.44 (CH_{Phen}-3,5), 129.29 (CH_{Bn}-3,5), 128.25 (CH_{Bn}-2,6), 127.15 (CH_{Bn}-4), 120.82 (CH_{Phen}-4), 114.59 (CH_{Phen}-2,6), 65.69 (CH_2OPh), 62.96 (CH_2Bn), 57.17 (CH_2N), 53.52 (CH_2-2-ppz, CH_2-6-ppz), 52.86 (CH_2-3-ppz, CH_2-5-ppz).

4.1.13.10. 4-Benzyl-1-(2-phenoxyethyl)piperidine (6b). The crude was purified by column chromatography (ratio:silica gel 1:50; CE:AcOEt 1:1). White solid, 70 mg (53% yield). ^1H NMR (400 MHz, $CDCl_3$) δ 7.20 (dd, J = 10.8, 4.8 Hz, 4H, CH_{Phen}-2,3,5,6), 7.11 (t, J = 7.3 Hz, 1H, CH_{Phen}-4), 7.06 (d, J = 7.2 Hz, 2H, CH_{Bn}-3,5), 6.87 (t, J = 7.3 Hz, 1H, CH_{Bn}-4), 6.82 (d, J = 8.3 Hz, 2H, CH_{Bn}-2,6), 4.08 (s, 2H, CH_2OPh), 2.97 (s, 2H, CH-2-ppd, CH-6-ppd), 2.78 (s, 2H, CH_2N), 2.48 (d, J = 6.9 Hz, 2H, CH_2Bn), 2.06 (s, 2H, CH-2′-ppd, CH-6′-ppd), 1.60 (d, J = 12.7 Hz, 2H, CH-3-ppd, CH-5-ppd), 1.54–1.44 (m, 1H, CH-4-ppd), 1.36 (s, 2H, CH-3′-ppd, CH-5′-ppd). ^{13}C NMR (101 MHz, $CDCl_3$) δ 158.50 (C_{Phen}-1), 140.47 (C_{Bn}-1), 129.45 (CH_{Phen}-3,5), 129.10 (CH_{Bn}-3,5), 128.28 (CH_{Bn}-2,6), 125.81 (CH_{Bn}-4), 120.81 (CH_{Phen}-4), 114.59 (CH_{Phen}-2,6), 65.53 (CH_2OPh), 57.46 (CH_2N), 54.35 (CH_2-2-ppd, CH_2-6-ppd), 43.02 (CH_2Bn), 37.56 (CH-4-ppd), 31.73 (CH_2-3-ppd, CH_2-5-ppd).

4.1.13.11. 1-Benzyl-4-(3-phenoxypropyl)piperazine (8a). The product was purified by column chromatography (crude: silica gel 1:80; DCM: MeOH 9:1). Yellow pale oil, 405 mg (56% yield). ^1H NMR (400 MHz, $CDCl_3$) δ 7.45–7.20 (m, 7H, CH_{Phen}-3,5, CH_{Bn}-2,3,4,5,6), 7.06–6.79 (m, 3H, CH_{Phen}-2,4,6), 4.26 (s, 2H, CH_2OPh), 4.02 (t, J = 7.6 Hz, 2H, CH_2Bn), 2.73–2.55 (m, 6H,CH-2-ppz, CH_2-3-ppz, CH_2-5-ppz, CH-6-ppz), 2.48 (t, J = 5.3 Hz, 4H, CH-2′-ppz, CH-6′-ppz, CH_2N), 1.84 (p, J = 7.6 Hz, 2H, $OCH_2CH_2CH_2N$).

4.1.13.12. 4-Benzyl-1-(3-phenoxypropyl)piperidine (8b). The product was purified by column chromatography (crude: silica gel 1:100; CE: AcOEt 1:1). Yellow pale oil, 175 mg (49% yield). ^1H NMR (400 MHz, $CDCl_3$) δ 7.33–7.27 (m, 4H, CH_{Bn}-3,5, CH_{Phen}-3,5), 7.22–7.15 (m, 3H, CH_{Bn}-2,4,6), 6.98–6.90 (m, 3H, CH_{Phen}-2,4,6), 4.10 (t, J = 4.8 Hz, 2H, PhenOCH_2), 3.00 (bdt, J = 12.5 Hz, 2H), 2.85 (t, J = 7.7 Hz, 2H, CH_2N), 2.55–2.43 (m, 2H, CH-2-ppd, CH-6-ppd), 2.01–1.83 (m, 4H, CH-2′-ppd, CH-6′-ppd, CH_2Bn), 1.72 (q, J = 6.9 Hz, 1H, CH-4-ppd), 1.68–1.41 (m, 4H, CH_2-3-ppd, CH_2-5-ppd). ^{13}C NMR (101 MHz, $CDCl_3$) δ 159.14 (C_{Phen}-1), 138.59 (C_{Bn}-1), 129.41 (CH_{Phen}-3,5), 129.04 (CH_{Bn}-3,5), 128.33 (CH_{Bn}-2,6), 126.29 (CH_{Bn}-4), 120.81 (CH_{Phen}-4), 114.46 (CH_{Phen}-2,6), 66.34 (CH_2OPh), 53.67 (CH_2N), 52.63 (CH_2-2-ppd, CH_2-6-ppd), 41.69 (CH_2Bn), 35.52 (CH-4-ppd), 30.28 (CH_2-3-ppd, CH_2-5-ppd), 27.28 (CH_2–CH_2–CH_2).

4.2. In vitro binding assay at SRs

The binding at S1R and S2R were performed as reported in literature [81,82]. [3H](+)pentazocine at 15 nM and [3H]DTG at 25 nM were used as hot radioligands for S1R and S2R, respectively. In S2R binding assay, 1 μM of cold (+)pentazocine was used to saturate the S1R binding site. The displacement of the radioligands upon incubation of SRs with the tested compounds was measured by scintillation counting. The results are expressed as a percent of inhibition of control specific binding, which is calculated as reported in (1), obtained in the presence of the test compounds

$$\%ofinhibition = 100 - \left(\frac{measuredspecificbinding}{controlspecificbinding} \bullet 100\right) \quad (1)$$

The IC_{50} values (concentration causing a half-maximal inhibition of control specific binding) and Hill coefficients (nH) were determined by non-linear regression analysis of the competition curves generated with mean replicate values using Hill equation curve fitting (2)

$$Y = D + \left(\frac{A - D}{1 + \left(\frac{C}{C_{50}}\right)^{nH}}\right) \quad (2)$$

where Y = specific binding, A = left asymptote of the curve, D = right asymptote of the curve, C = compound concentration, C_{50} = IC_{50}, and nH = slope factor. This analysis was performed using software developed at Cerep (Hill software) and validated by comparison with data generated by the commercial software SigmaPlot® 4.0 for Windows® (© 1997 by SPSS Inc.). The inhibition constants (k_i) were calculated using the Cheng Prusoff equation (3)

$$k_i = \left(\frac{IC_{50}}{1 + \frac{L}{K_D}}\right) \quad (3)$$

where L = concentration of radioligand in the assay, and K_D = affinity of the radioligand for the receptor. A scatchard plot is used to determine the K_D.

4.3. In vitro binding assay at NMDA receptor

The binding at NMDA receptor was performed as reported in literature [83]. [^{3}H]CGP39653, an NMDA antagonist, at 5 nM was used as radioligands. The displacement of the radioligand upon incubation of NMDAR with the tested compounds was measured by scintillation counting. The results are expressed as a percent of inhibition of control specific binding, which is calculated as reported in (1).

4.4. Cellular assay for neuroprotection activity

The neuroprotective capacity of the compounds was assessed according to Benchekroun et al. The human neuroblastoma SH-SY5Y cells were maintained in Dulbecco's modified Eagle's medium (DMEM) supplemented with 10% fetal bovine serum (FBS), 2 mM L-glutamine, 50 U/ml penicillin and 50 mg/mL streptomycin in a humid atmosphere of 95% air and 5% CO2 at 37 °C. Prior to cell treatment, the medium was replaced with fresh medium containing the test compounds (0.1–100 μM concentration) using a reduced serum medium (2% FBS). The test compounds were prepared as 10 mM stock solutions in DMSO. In the neuroprotection assay, SH-SY5Y cells were co-incubated with NMDA at a concentration of 250 μM, oligomycin at a concentration of 2.5 μM or rotenone at a concentration of 25 μM and tested compounds at different concentrations. Cell viability assay The number of living cells was evaluated by the 3-(4,5-dimethylthiazol-2-yl)-2,5-diphenyltetrazolium bromide (MTT) assay.10 Briefly, 100 μL of cell suspension were plated in 96-well plates at a density of ~7000 cells/well. After one day incubation at 37 °C in a humid atmosphere with 5% CO2, the culture medium was replaced with 100 μL of fresh medium or medium containing different concentrations of the test compounds. Untreated cells were used as positive control. After the incubation period of 24 h, 10 μL of a 0.5% (w/v) MTT/PBS solution were added to each well and the incubation was prolonged for 2 h. After this period, the medium was removed and

replaced with 100 μL of DMSO. The absorbance of the individual well was measured by a microplate reader (Wallac Victor3, 1420 Multilabel Counter, PerkinElmer). Each compound concentration was tested in triplicate, and results presented as percentage of the control value. For the neuroprotection assay, SH-SY5Y cells were seeded in 96-well plates at the same density used for cytotoxicity assay. Cells were exposed for 24 h to NMDA, rotenone or oligomycin in the absence or presence of test compounds at concentrations ranging from 0.1 to 5 μM at 37 °C. The neuroprotective capacity of the compounds was assessed in the same conditions described above and in the presence of 4-methyl-1-[4-(6-methoxynaphthalen-1-yl)butyl]piperidine (PB212). Briefly, SHSY5Y cells were pre-incubated for 1 h with PB212 (5 μM, non-toxic dose) and then treated with the combination of compounds (1 μM or 5 μM)/PB212 (5 μM)/rotenone (25 μM) or NMDA (250 μM). The cell viability was evaluated by MTT assay. Data are presented as the mean ± SEM. Statistical comparisons were performed by two-way ANOVA followed by Bonferroni post hoc test using the statistical package in the GraphPad Prism software v. 5.01; values of *$p < 0.05$, **$p < 0.01$, ***$p < 0.001$ vs NMDA, rotenone or oligomycin alone were considered statistically significant.

4.5. Cell culture

LoVo colon cancer cells, A549 lung cancer cells and Panc-1 pancreas cancer cells (ATCC®, Manassa VA, USA) were grown in Ham's F–12K Medium and DMEM (ATCC®, Manassa VA, USA) supplemented with 10% Foetal Bovine Serum (FBS) (Euroclone) sterile filtered. All experiments were performed on cells in the exponential growth phase and checked periodically.

4.6. Cell proliferation assay

Cytotoxicity was assayed using CellTiter 96® AQ_{ueous} One Solution Cell Proliferation Assay according to manufacturing's instructions (Promega, Milan, Italy).

Briefly, cells were seeded onto a 96-well plate at a density of 2500 cells/well. Cell lines were exposed to increasing concentrations of the drug, ranging from 0.1 to 100 μM. The effect of the drugs was evaluated after 24, 48, 72 h of continued exposure. Three independent experiments were performed in quadruplicate. The optical density of treated and untreated cells was determined at a wavelength of 490 nm using a fluorescence plate reader (Synergy H1 microplate reader, BioTek, USA). Data were processed using GraphPad Prism 8 program (version 8.3.0).

4.7. RealTime RT-qPCR

TRIzol reagent (Life Technologies, Carlsbad, CA, USA) was used, following the manufacturer's instructions, for total cellular RNA extraction. RNA was quantified by Nanodrop MD-1000 spectrophotometer system. iScript cDNA Synthesis kit (Bio-Rad Laboratories, Hercules, CA, USA) was used to perform reverse transcription reactions. 400 ng of total RNA were retrotranscribed in 20 μL of nuclease-free water. Real-time PCR was performed by a 7500 Fast Real-Time PCR system (Applied Biosystems, Foster City, CA, USA), and the expression of SIGMA 1 and TMEM-97 genes were detected by TaqMan assays. Reactions containing 40 ng of cDNA template, TaqMan Universal PCR Master Mix (2X), and selected TaqMan assays (20X) were carried out in triplicate at a final volume of 20 μL. Samples were maintained at 50 °C for 2 min, then at 95 °C for 10 min followed by 40 amplification cycles at 95 °C for 15 s, and 60 °C for 30 s. The changes in gene expression were displayed relative to a control sample (U87 brain tumor cell line, ATCC), demonstrated to express the genes. Gene expression was normalized with two endogenous reference genes, GAPDH and HPRT, identified as the most stable genes by the geNorm VBA applet for Microsoft Excel. Data are reported as mean ± SD. Data were processed using the GraphPad Prism program (version 8.3.0) (GraphPad Software).

4.8. Animal care and maintenance

Tg(GFAP:GFP) zebrafish (*Danio rerio*) were a kind gift from Department of Biology, University of Padova (Italy) and maintained in a recirculatory system at 28 °C in a light/dark cycle of 14/10 h. They were fed thrice a day with dry food and Artemia. Zebrafish embryos and larvae until 5 days post fertilization (dpf) were used for the experiments, mating between 2 females and 1 male were set up the day before the test. Eggs were preserved from predation by adult fish using a plastic separator in the tanks. Eggs were collected right after spawning and used in the teratogenicity experiments. Zebrafish husbandry procedures were performed according to the Directive 2010/63/EU and in compliance with local animal welfare regulations (authorization n. prot. 18,311/2016; released by the "Comune di Meldola", November 9, 2016).

4.9. Teratogenic test

Teratogenic test was performed as previously reported (Harris C. et al. Book of developmental toxicology, Springer Science and Business Media, LLC 2012). Briefly, Eggs were collected, rinse out with embryo medium (for 1L of distilled water: 0.1 g sodium bicarbonate, 0.1 g instant ocean, 0.19 g calcium sulfate) and put in different petri dishes with the same medium, only unscathed embryos were selected. Generally, 8 embryos per untreated control, and treatment concentrations were cultured. Eggs were treated with increasing concentration of PL16 and PL24 compounds respectively starting from 1 h post-fertilization. They were incubated at 28 °C for about 5 days (without changing the media) in order to allow exposure to compounds throughout all development stages. Teratogenic effects were evaluated after 5 days from treatment with morphological and viability observations. The experiment was performed in octuplicate, and data were assessed using a sample score sheet as reported by Brannen KC and collegues (Development of a zebrafish embryo teratogenicity assay and quantitative prediction model. Birth Defects Research Part B, vol 89, issue 1, 2010) and in supplementary methods (Tables S1 and S2).

4.10. Solubility studies

The buffer solutions were HCl/KCl for pH 1.2, KH2PO4/NaOH for pH 6.8, and KH2PO4/Na2HPO4 for pH 7.4.20 μL of a 10 mM DMSO solution of the compounds was diluted in 1980 μL of the appropriate buffer solution to achieve a maximum theoretical concentration of 30,700 μg/mL and 29,500 μg/mL for compounds 6b and 8b, respectively, and a 1% v/v final concentration in DMSO. The solutions were incubated for 24 h at 1200 rpm. After incubation, the suspension was filtered using hydrophilic polycarbonate filter membrane (pore size 0.45 μm, thickness 17–22 μm). Filtrate solutions were diluted 1 : 1 with MeOH to avoid further precipitation and analysed.

Declaration of competing interest

The authors declare that they have no known competing financial interests or personal relationships that could have appeared to influence the work reported in this paper.

Data availability

Data will be made available on request.

Acknowledgments

This research work has received funding from the University of Modena and Reggio Emilia by the project "SMILE: Sigma1 ligands for Memory loss and Impaired Learning" FONDO DI ATENEO PER LA RICERCA JUNIOR ANNO 2018 - FAR2018, Italy (A.006@FAR2018JUNIOR@05FA-LINCIANO_FAR18J- (0.20) CUP E56C18002080001).

Appendix A. Supplementary data

Supplementary data to this article can be found online at https://doi.org/10.1016/j.ejmech.2023.115163.

References

[1] R.N.L. Lamptey, B. Chaulagain, R. Trivedi, A. Gothwal, B. Layek, J. Singh, A review of the common neurodegenerative disorders: current therapeutic approaches and the potential role of nanotherapeutics, Int. J. Mol. Sci. 23 (2022) 1851, https://doi.org/10.3390/ijms23031851.

[2] B.N. Dugger, D.W. Dickson, Pathology of neurodegenerative diseases, Cold Spring Harbor Perspect. Biol. 9 (2017), a028035, https://doi.org/10.1101/cshperspect.a028035.

[3] D.E. Rollins, D.K. Blumenthal, Drug therapy of neurodegenerative diseases, in: Workb. Caseb. Goodman Gilman's Pharmacol. Basis Ther., McGraw-Hill Education, New York, NY, 2016. http://accesspharmacy.mhmedical.com/content.aspx?aid=1121942754.

[4] P. Maresova, J. Hruska, B. Klimova, S. Barakovic, O. Krejcar, Activities of daily living and associated costs in the most widespread neurodegenerative diseases: a systematic review, Clin. Interv. Aging 15 (2020) 1841–1862, https://doi.org/10.2147/CIA.S264688.

[5] WHO, 10 facts on ageing and health (n.d.), https://www.who.int/news-room/fact-sheets/detail/10-facts-on-ageing-and-health. (Accessed 5 September 2022).

[6] J. Cummings, Disease modification and Neuroprotection in neurodegenerative disorders, Transl. Neurodegener. 6 (2017) 25, https://doi.org/10.1186/s40035-017-0096-2.

[7] A.V. Morant, V. Jagalski, H.T. Vestergaard, Labeling of disease-modifying therapies for neurodegenerative disorders, Front. Med. 6 (2019), https://doi.org/10.3389/fmed.2019.00223.

[8] L. Nguyen, B.P. Lucke-Wold, S.A. Mookerjee, J.Z. Cavendish, M.J. Robson, A. L. Scandinaro, R.R. Matsumoto, Role of sigma-1 receptors in neurodegenerative diseases, J. Pharmacol. Sci. 127 (2015) 17–29, https://doi.org/10.1016/j.jphs.2014.12.005.

[9] K. Sałaciak, K. Pytka, Revisiting the sigma-1 receptor as a biological target to treat affective and cognitive disorders, Neurosci. Biobehav. Rev. 132 (2022) 1114–1136, https://doi.org/10.1016/j.neubiorev.2021.10.037.

[10] A. Piechal, A. Jakimiuk, D. Mirowska-Guzel, Sigma receptors and neurological disorders, Pharmacol. Rep. 73 (2021) 1582–1594, https://doi.org/10.1007/s43440-021-00310-7.

[11] G.E. Thomas, M. Szücs, J.Y. Mamone, W.T. Bem, M.D. Rush, F.E. Johnson, C. J. Coscia, Sigma and opioid receptors in human brain tumors, Life Sci. 46 (1990) 1279–1286, https://doi.org/10.1016/0024-3205(90)90360-4.

[12] B.J. Vilner, C.S. John, W.D. Bowen, Sigma-1 and sigma-2 receptors are expressed in a wide variety of human and rodent tumor cell lines, Cancer Res. 55 (1995) 408–413. http://www.ncbi.nlm.nih.gov/pubmed/7812973.

[13] M. Cortesi, A. Zamagni, S. Pignatta, M. Zanoni, C. Arienti, D. Rossi, S. Collina, A. Tesei, Pan-sigma receptor modulator RC-106 induces terminal unfolded protein response in in vitro pancreatic cancer model, Int. J. Mol. Sci. 21 (2020) 9012, https://doi.org/10.3390/ijms21239012.

[14] G. Rossino, M. Rui, P. Linciano, D. Rossi, M. Boiocchi, M. Peviani, E. Poggio, D. Curti, D. Schepmann, B. Wünsch, M. González-Avendaño, A. Vergara-Jaque, J. Caballero, S. Collina, Bitopic sigma 1 receptor modulators to shed light on molecular mechanisms underpinning ligand binding and receptor oligomerization, J. Med. Chem. 64 (2021) 14997–15016, https://doi.org/10.1021/acs.jmedchem.1c00886.

[15] M. Pabba, A.Y.C. Wong, N. Ahlskog, E. Hristova, D. Biscaro, W. Nassrallah, J. K. Ngsee, M. Snyder, J.-C. Beique, R. Bergeron, NMDA receptors are upregulated and trafficked to the plasma membrane after sigma-1 receptor activation in the rat hippocampus, J. Neurosci. 34 (2014) 11325–11338, https://doi.org/10.1523/JNEUROSCI.0458-14.2014.

[16] T. Goyagi, S. Goto, A. Bhardwaj, V.L. Dawson, P.D. Hurn, J.R. Kirsch, Neuroprotective effect of σ 1 -receptor ligand 4-phenyl-1-(4-phenylbutyl) piperidine (PPBP) is linked to reduced neuronal nitric oxide production, Stroke 32 (2001) 1613–1620, https://doi.org/10.1161/01.STR.32.7.1613.

[17] Z.-J. Yang, E.L. Carter, M.T. Torbey, L.J. Martin, R.C. Koehler, Sigma receptor ligand 4-phenyl-1-(4-phenylbutyl)-piperidine modulates neuronal nitric oxide synthase/postsynaptic density-95 coupling mechanisms and protects against neonatal ischemic degeneration of striatal neurons, Exp. Neurol. 221 (2010) 166–174, https://doi.org/10.1016/j.expneurol.2009.10.019.

[18] G. Pellavio, G. Rossino, G. Gastaldi, D. Rossi, P. Linciano, S. Collina, U. Laforenza, Sigma-1 receptor agonists acting on aquaporin-mediated H2O2 permeability: new tools for counteracting oxidative stress, Int. J. Mol. Sci. 22 (2021) 9790, https://doi.org/10.3390/ijms22189790.

[19] C. Xu, B. Bailly-Maitre, J.C. Reed, Endoplasmic reticulum stress: cell life and death decisions, J. Clin. Invest. 115 (2005) 2656–2664, https://doi.org/10.1172/JCI26373.

[20] A. Tesei, M. Cortesi, A. Zamagni, C. Arienti, S. Pignatta, M. Zanoni, M. Paolillo, D. Curti, M. Rui, D. Rossi, S. Collina, Sigma receptors as endoplasmic reticulum stress "gatekeepers" and their modulators as emerging new weapons in the fight against cancer, Front. Pharmacol. 9 (2018) 711, https://doi.org/10.3389/fphar.2018.00711.

[21] M. Moenner, O. Pluquet, M. Bouchecareilh, E. Chevet, Integrated endoplasmic reticulum stress responses in cancer, Cancer Res. 67 (2007) 10631–10634, https://doi.org/10.1158/0008-5472.CAN-07-1705.

[22] M.K. Brown, N. Naidoo, The endoplasmic reticulum stress response in aging and age-related diseases, Front. Physiol. 3 (2012) 263, https://doi.org/10.3389/fphys.2012.00263.

[23] A.H. Schonthal, Targeting endoplasmic reticulum stress for cancer therapy, Front. Biosci. 4 (2012) 412–431, https://doi.org/10.2741/276.

[24] R.K. Yadav, S.-W. Chae, H.-R. Kim, H.J. Chae, Endoplasmic reticulum stress and cancer, J. Cancer Prev. 19 (2014) 75–88, https://doi.org/10.15430/JCP.2014.19.2.75.

[25] J. Jia, J. Cheng, C. Wang, X. Zhen, Sigma-1 receptor-modulated neuroinflammation in neurological diseases, Front. Cell. Neurosci. 12 (2018) 314, https://doi.org/10.3389/fncel.2018.00314.

[26] D. Rossi, A. Marra, P. Picconi, M. Serra, L. Catenacci, M. Sorrenti, E. Laurini, M. Fermeglia, S. Pricl, S. Brambilla, N. Almirante, M. Peviani, D. Curti, S. Collina, Identification of RC-33 as a potent and selective σ1 receptor agonist potentiating NGF-induced neurite outgrowth in PC12 cells. Part 2: g-Scale synthesis, physicochemical characterization and in vitro metabolic stability, Bioorg. Med. Chem. 21 (2013) 2577–2586, https://doi.org/10.1016/j.bmc.2013.02.029.

[27] D. Rossi, A. Pedrali, M. Urbano, R. Gaggeri, M. Serra, L. Fernández, M. Fernández, J. Caballero, S. Ronsisvalle, O. Prezzavento, D. Schepmann, B. Wuensch, M. Peviani, D. Curti, O. Azzolina, S. Collina, Identification of a potent and selective σ1 receptor agonist potentiating NGF-induced neurite outgrowth in PC12 cells, Bioorg. Med. Chem. 19 (2011) 6210–6224, https://doi.org/10.1016/j.bmc.2011.09.016.

[28] F. Bogár, L. Fülöp, B. Penke, Novel therapeutic target for prevention of neurodegenerative diseases: modulation of neuroinflammation with sig-1R ligands, Biomolecules 12 (2022) 363, https://doi.org/10.3390/biom12030363.

[29] W.-H. Ma, A.-F. Chen, X.-Y. Xie, Y.-S. Huang, Sigma ligands as potent inhibitors of Aβ and AβOs in neurons and promising therapeutic agents of Alzheimer's disease, Neuropharmacology 190 (2021), 108342, https://doi.org/10.1016/j.neuropharm.2020.108342.

[30] J.-L. Jin, M. Fang, Y.-X. Zhao, X.-Y. Liu, Roles of sigma-1 receptors in Alzheimer's disease, Int. J. Clin. Exp. Med. 8 (2015) 4808–4820. http://www.ncbi.nlm.nih.gov/pubmed/26131055.

[31] G. Rossino, M. Rui, L. Pozzetti, D. Schepmann, B. Wünsch, D. Zampieri, G. Pellavio, U. Laforenza, S. Rinaldi, G. Colombo, L. Morelli, P. Linciano, D. Rossi, S. Collina, Setup and validation of a reliable docking protocol for the development of neuroprotective agents by targeting the sigma-1 receptor (S1R), Int. J. Mol. Sci. 21 (2020) 7708, https://doi.org/10.3390/ijms21207708.

[32] B. Vigani, S. Rossi, G. Sandri, M.C. Bonferoni, M. Rui, S. Collina, F. Fagiani, C. Lanni, F. Ferrari, Dual-functioning scaffolds for the treatment of spinal cord injury: alginate nanofibers loaded with the sigma 1 receptor (S1R) agonist RC-33 in chitosan films, Mar. Drugs 18 (2019) 21, https://doi.org/10.3390/md18010021.

[33] D. Zampieri, S. Fortuna, A. Calabretti, M. Romano, R. Menegazzi, D. Schepmann, B. Wünsch, S. Collina, D. Zanon, M.G. Mamolo, Discovery of new potent dual sigma receptor/GluN2b ligands with antioxidant property as neuroprotective agents, Eur. J. Med. Chem. 180 (2019) 268–282, https://doi.org/10.1016/j.ejmech.2019.07.012.

[34] J.L. Velázquez-Libera, G. Rossino, C. Navarro-Retamal, S. Collina, J. Caballero, Docking, interaction fingerprint, and three-dimensional quantitative structure–activity relationship (3D-QSAR) of Sigma1 receptor ligands, analogs of the neuroprotective agent RC-33, Front. Chem. 7 (2019), https://doi.org/10.3389/fchem.2019.00496.

[35] M. Rui, G. Rossino, D. Rossi, S. Collina, CHAPTER 12. Sigma Receptors as New Target for Multiple Sclerosis, 2019, pp. 264–284, https://doi.org/10.1039/9781788016070-00264.

[36] M. Rui, G. Rossino, S. Coniglio, S. Monteleone, A. Scuteri, A. Malacrida, D. Rossi, L. Catenacci, M. Sorrenti, M. Paolillo, D. Curti, L. Venturini, D. Schepmann, B. Wünsch, K.R. Liedl, G. Cavaletti, V. Pace, E. Urban, S. Collina, Identification of dual Sigma1 receptor modulators/acetylcholinesterase inhibitors with antioxidant and neurotrophic properties, as neuroprotective agents, Eur. J. Med. Chem. 158 (2018) 353–370, https://doi.org/10.1016/j.ejmech.2018.09.010.

[37] S. Collina, M. Rui, S. Stotani, E. Bignardi, D. Rossi, D. Curti, F. Giordanetto, A. Malacrida, A. Scuteri, G. Cavaletti, Are sigma receptor modulators a weapon against multiple sclerosis disease? Future Med. Chem. 9 (2017) 2029–2051, https://doi.org/10.4155/fmc-2017-0122.

[38] D. Rossi, A. Pedrali, A. Marra, L. Pignataro, D. Schepmann, B. Wünsch, L. Ye, K. Leuner, M. Peviani, D. Curti, O. Azzolina, S. Collina, Studies on the enantiomers of as neuroprotective agents: isolation, configurational assignment, and preliminary biological profile, Chirality 25 (2013) 814–822, https://doi.org/10.1002/chir.22223.

[39] V. Villard, J. Espallergues, E. Keller, A. Vamvakides, T. Maurice, Anti-amnesic and neuroprotective potentials of the mixed muscarinic receptor/sigma1 (σ1) ligand ANAVEX2-73, a novel aminotetrahydrofuran derivative, J. Psychopharmacol. 25 (2011) 1101–1117, https://doi.org/10.1177/0269881110379286.

[40] J. Cummings, G. Lee, K. Zhong, J. Fonseca, K. Taghva, Alzheimer's disease drug development pipeline: 2021, Alzheimer's Dement. Transl. Res. Clin. Interv. 7 (2021), https://doi.org/10.1002/trc2.12179.

[41] C. Sun, M.J. Armstrong, Treatment of Parkinson's disease with cognitive impairment: current approaches and future directions, Behav. Sci. 11 (2021) 54, https://doi.org/10.3390/bs11040054.

[42] AdisInsight drugs, blarcamesine - anavex life sciences (n.d.), https://adis.springer.com/drugs/800033840. (Accessed 28 September 2022).

[43] W.E. Kaufmann, J. Sprouse, N. Rebowe, T. Hanania, D. Klamer, C.U. Missling, ANAVEX®2-73 (blarcamesine), a Sigma-1 receptor agonist, ameliorates neurologic impairments in a mouse model of Rett syndrome, Pharmacol. Biochem. Behav. 187 (2019), 172796, https://doi.org/10.1016/j.pbb.2019.172796.

[44] AdisInsight drugs, cutamesine (n.d.), https://adisinsight.springer.com/drugs/800007486. (Accessed 28 September 2022).

[45] V. Francardo, M. Geva, F. Bez, Q. Denis, L. Steiner, M.R. Hayden, M.A. Cenci, Pridopidine induces functional neurorestoration via the sigma-1 receptor in a mouse model of Parkinson's disease, Neurotherapeutics (2019) 465–479, https://doi.org/10.1007/s13311-018-00699-9.

[46] AdisInsight drugs, pridopidine - prilenia therapeutics (n.d.), https://adisinsight.springer.com/drugs/800017494. (Accessed 28 September 2022).

[47] S. Chen, T. Liang, T. Xue, S. Xue, Q. Xue, Pridopidine for the improvement of motor function in patients with Huntington's disease: a systematic review and meta-analysis of randomized controlled trials, Front. Neurol. 12 (2021), https://doi.org/10.3389/fneur.2021.658123.

[48] S. Franchini, U.M. Battisti, A. Prandi, A. Tait, C. Borsari, E. Cichero, P. Fossa, A. Cilia, O. Prezzavento, S. Ronsisvalle, G. Aricò, C. Parenti, L. Brasili, Scouting new sigma receptor ligands: synthesis, pharmacological evaluation and molecular modeling of 1,3-dioxolane-based structures and derivatives, Eur. J. Med. Chem. 112 (2016) 1–19, https://doi.org/10.1016/j.ejmech.2016.01.059.

[49] S. Franchini, C. Sorbi, U.M. Battisti, A. Tait, L.I. Bencheva, E. Cichero, P. Fossa, A. Cilia, O. Prezzavento, S. Ronsisvalle, G. Aricò, L. Benassi, C. Vaschieri, P. Azzoni, C. Magnoni, L. Brasili, Structure–activity relationships within a series of σ1 and σ2 receptor ligands: identification of a σ2 receptor agonist (BS148) with selective toxicity against metastatic melanoma, ChemMedChem 12 (2017) 1893–1905, https://doi.org/10.1002/cmdc.201700427.

[50] L. Costantino, F. Gandolfi, C. Sorbi, S. Franchini, O. Prezzavento, F. Vittorio, G. Ronsisvalle, A. Leonardi, E. Poggesi, L. Brasili, Synthesis and structure-activity relationships of 1-aralkyl-4- benzylpiperidine and 1-aralkyl-4-benzylpiperazine derivatives as potent σ ligands, J. Med. Chem. 48 (2005) 266–273, https://doi.org/10.1021/jm049433t.

[51] S. Franchini, P. Linciano, G. Puja, A. Tait, C. Borsari, N. Denora, R.M. Iacobazzi, L. Brasili, C. Sorbi, Novel dithiolane-based ligands combining sigma and NMDA receptor interactions as potential neuroprotective agents, ACS Med. Chem. Lett. (2020), https://doi.org/10.1021/acsmedchemlett.0c00129.

[52] R. Pascual, C. Almansa, C. Plata-Salamán, J.M. Vela, A new pharmacophore model for the design of sigma-1 ligands validated on a large experimental dataset, Front. Pharmacol. 10 (2019) 1–16, https://doi.org/10.3389/fphar.2019.00519.

[53] A. Daina, O. Michielin, V. Zoete, SwissADME: a free web tool to evaluate pharmacokinetics, drug-likeness and medicinal chemistry friendliness of small molecules, Sci. Rep. 7 (2017), 42717, https://doi.org/10.1038/srep42717.

[54] H. Pajouhesh, G.R. Lenz, Medicinal chemical properties of successful central nervous system drugs, NeuroRx 2 (2005) 541–553, https://doi.org/10.1602/neurorx.2.4.541.

[55] Z. Rankovic, CNS drug design: balancing physicochemical properties for optimal brain exposure, J. Med. Chem. 58 (2015) 2584–2608, https://doi.org/10.1021/jm501535r.

[56] D. Lagorce, O. Sperandio, H. Galons, M.A. Miteva, B.O. Villoutreix, FAF-Drugs2: free ADME/tox filtering tool to assist drug discovery and chemical biology projects, BMC Bioinf. 9 (2008), https://doi.org/10.1186/1471-2105-9-396.

[57] L. Giampietro, A. D'Angelo, A. Giancristofaro, A. Ammazzalorso, B. De Filippis, M. Di Matteo, M. Fantacuzzi, P. Linciano, C. Maccallini, R. Amoroso, Effect of stilbene and chalcone scaffolds incorporation in clofibric acid on PPARα agonistic activity, Med. Chem. 10 (2014) 59–65. http://www.ncbi.nlm.nih.gov/pubmed/23432317.

[58] S. Franchini, C. Sorbi, P. Linciano, G. Carnevale, A. Tait, S. Ronsisvalle, M. Buccioni, F. Del Bello, A. Cilia, L. Pirona, N. De Nora, R.M. Iacobazzi, L. Brasili, 1,3-Dioxane as a scaffold for potent and selective 5-HT1AR agonist with in-vivo anxiolytic, anti-depressant and anti-nociceptive activity, Eur. J. Med. Chem. 176 (2019) 310–325, https://doi.org/10.1016/j.ejmech.2019.05.024.

[59] T. Ishima, T. Nishimura, M. Iyo, K. Hashimoto, Potentiation of nerve growth factor-induced neurite outgrowth in PC12 cells by donepezil: role of sigma-1 receptors and IP3 receptors, Prog. Neuro Psychopharmacol. Biol. Psychiatr. 32 (2008) 1656–1659, https://doi.org/10.1016/j.pnpbp.2008.06.011.

[60] D. Rossi, A. Pedrali, R. Gaggeri, A. Marra, L. Pignataro, E. Laurini, V. Dal Col, M. Fermeglia, S. Pricl, D. Schepmann, B. Wünsch, M. Peviani, D. Curti, S. Collina, Chemical, pharmacological, and in vitro metabolic stability studies on enantiomerically pure RC-33 compounds: promising neuroprotective agents acting as σ 1 receptor agonists, ChemMedChem 8 (2013) 1514–1527, https://doi.org/10.1002/cmdc.201300218.

[61] A. Marra, D. Rossi, L. Pignataro, C. Bigogno, A. Canta, N. Oggioni, A. Malacrida, M. Corbo, G. Cavaletti, M. Peviani, D. Curti, G. Dondio, S. Collina, Toward the identification of neuroprotective agents: g-scale synthesis, pharmacokinetic evaluation and CNS distribution of (R)-RC-33, a promising Sigma1 receptor agonist, Future Med. Chem. 8 (2016) 287–295, https://doi.org/10.4155/fmc.15.191.

[62] Y. Kimura, Y. Fujita, K. Shibata, M. Mori, T. Yamashita, Sigma-1 receptor enhances neurite elongation of cerebellar granule neurons via TrkB signaling, PLoS One 8 (2013), e75760, https://doi.org/10.1371/journal.pone.0075760.

[63] A. Slanzi, G. Iannoto, B. Rossi, E. Zenaro, G. Constantin, In vitro models of neurodegenerative diseases, Front. Cell Dev. Biol. 8 (2020), https://doi.org/10.3389/fcell.2020.00328.

[64] N. Xiong, X. Long, J. Xiong, M. Jia, C. Chen, J. Huang, D. Ghoorah, X. Kong, Z. Lin, T. Wang, Mitochondrial complex I inhibitor rotenone-induced toxicity and its potential mechanisms in Parkinson's disease models, Crit. Rev. Toxicol. 42 (2012) 613–632, https://doi.org/10.3109/10408444.2012.680431.

[65] N.M.C. Connolly, P. Theurey, V. Adam-Vizi, N.G. Bazan, P. Bernardi, J.P. Bolaños, C. Culmsee, V.L. Dawson, M. Deshmukh, M.R. Duchen, H. Düssmann, G. Fiskum, M.F. Galindo, G.E. Hardingham, J.M. Hardwick, M.B. Jekabsons, E.A. Jonas, J. Jordán, S.A. Lipton, G. Manfredi, M.P. Mattson, B. McLaughlin, A. Methner, A. N. Murphy, M.P. Murphy, D.G. Nicholls, B.M. Polster, T. Pozzan, R. Rizzuto, J. Satrústegui, R.S. Slack, R.A. Swanson, R.H. Swerdlow, Y. Will, Z. Ying, A. Joselin, A. Gioran, C. Moreira Pinho, O. Watters, M. Salvucci, I. Llorente-Folch, D.S. Park, D. Bano, M. Ankarcrona, P. Pizzo, J.H.M. Prehn, Guidelines on experimental methods to assess mitochondrial dysfunction in cellular models of neurodegenerative diseases, Cell Death Differ. 25 (2018) 542–572, https://doi.org/10.1038/s41418-017-0020-4.

[66] R. Betarbet, T.B. Sherer, J.T. Greenamyre, Animal models of Parkinson's disease, Bioessays 24 (2002) 308–318, https://doi.org/10.1002/bies.10067.

[67] R.F. Simões, R. Ferrão, M.R. Silva, S.L.C. Pinho, L. Ferreira, P.J. Oliveira, T. Cunha-Oliveira, Refinement of a differentiation protocol using neuroblastoma SH-SY5Y cells for use in neurotoxicology research, Food Chem. Toxicol. 149 (2021), 111967, https://doi.org/10.1016/j.fct.2021.111967.

[68] R.F. Simões, P.J. Oliveira, T. Cunha-Oliveira, F.B. Pereira, Evaluation of 6-hydroxydopamine and rotenone in vitro neurotoxicity on differentiated SH-SY5Y cells using applied computational statistics, Int. J. Mol. Sci. 23 (2022) 3009, https://doi.org/10.3390/ijms23063009.

[69] C. Abate, C. Riganti, M.L. Pati, D. Ghigo, F. Berardi, T. Mavlyutov, L.-W. Guo, A. Ruoho, Development of sigma-1 (σ 1) receptor fluorescent ligands as versatile tools to study σ 1 receptors, Eur. J. Med. Chem. 108 (2016) 577–585, https://doi.org/10.1016/j.ejmech.2015.12.014.

[70] W.J. Geldenhuys, A.S. Darvesh, Pharmacotherapy of Alzheimer's disease: current and future trends, Expert Rev. Neurother. 15 (2015) 3–5, https://doi.org/10.1586/14737175.2015.990884.

[71] United States Pharmacopeial, General Notices and Requirements. Description and Solubility, 2015.

[72] P. Linciano, B. De Filippis, A. Ammazzalorso, P. Amoia, M. Fantacuzzi, L. Giampietro, C. Maccallini, C. Petit, R. Amoroso, Druggability Profile of Stilbene-Derived PPAR Agonists : Determination of Physicochemical Properties and PAMPA Druggability Profile of Stilbene-Derived PPAR Agonists : Determination of Physicochemical Properties and PAMPA Study, Medchemcomm, 2019 (Accepted Manuscript).

[73] J.-M. Cardot, A. Garcia Arieta, P. Paixao, I. Tasevska, B. Davit, Implementing the biopharmaceutics classification system in drug development: reconciling similarities, differences, and shared challenges in the EMA and US-FDA-recommended approaches, AAPS J. 18 (2016) 1039–1046, https://doi.org/10.1208/s12248-016-9915-0.

[74] M.U. Mehta, R.S. Uppoor, D.P. Conner, P. Seo, J. Vaidyanathan, D.A. Volpe, E. Stier, D. Chilukuri, A. Dorantes, T. Ghosh, H. Mandula, K. Raines, P. Dhanormchitphong, J. Woodcock, L.X. Yu, Impact of the US FDA "biopharmaceutics classification system" (BCS) guidance on global drug development, Mol. Pharm. 14 (2017) 4334–4338, https://doi.org/10.1021/acs.molpharmaceut.7b00687.

[75] S. Cassar, I. Adatto, J.L. Freeman, J.T. Gamse, I. Iturria, C. Lawrence, A. Muriana, R.T. Peterson, S. Van Cruchten, L.I. Zon, Use of zebrafish in drug discovery toxicology, Chem. Res. Toxicol. 33 (2020) 95–118, https://doi.org/10.1021/acs.chemrestox.9b00335.

[76] S. Padilla, S. Glaberman, The zebrafish (Danio rerio) model in toxicity testing, in: An Introd. To Interdiscip. Toxicol., Elsevier, 2020, pp. 525–532, https://doi.org/10.1016/B978-0-12-813602-7.00037-5.

[77] C. Harris, J.M. Hansen (Eds.), Developmental Toxicology, Humana Press, Totowa, NJ, 2012, https://doi.org/10.1007/978-1-61779-867-2.

[78] R. Bergeron, C. de Montigny, G. Debonnel, Biphasic effects of sigma ligands on the neuronal response to N-methyl-D-aspartate, Naunyn-Schmiedeberg's Arch. Pharmacol. 351 (1995) 252–260, https://doi.org/10.1007/BF00233244.

[79] X. Liang, R.Y. Wang, Biphasic modulatory action of the selective sigma receptor ligand SR 31742A on N-methyl-D-aspartate-induced neuronal responses in the frontal cortex, Brain Res. 807 (1998) 208–213, https://doi.org/10.1016/s0006-8993(98)00797-5.

[80] E.J. Fletcher, J. Church, K. Abdel-Hamid, J.F. MacDonald, Blockade by sigma site ligands of N-methyl-D-aspartate-evoked responses in rat and mouse cultured hippocampal pyramidal neurones, Br. J. Pharmacol. 116 (1995) 2791–2800, https://doi.org/10.1111/j.1476-5381.1995.tb15928.x.

[81] M.E. Ganapathy, P.D. Prasad, W. Huang, P. Seth, F.H. Leibach, V. Ganapathy, Molecular and ligand-binding characterization of the σ-receptor in the Jurkat human T lymphocyte cell line, J. Pharmacol. Exp. Therapeut. 289 (1999) 251–260.

[82] R. Kekuda, P.D. Prasad, Y.-J. Fei, F.H. Leibach, V. Ganapathy, Cloning and functional expression of the human type 1 sigma receptor (hSigmaR1), Biochem. Biophys. Res. Commun. 229 (1996) 553–558, https://doi.org/10.1006/bbrc.1996.1842.

[83] M.A. Sills, G. Fagg, M. Pozza, C. Angst, D.E. Brundish, S.D. Hurt, E. Jay Wilusz, M. Williams, [3H]CGP 39653: a new N-methyl-D-aspartate antagonist radioligand with low nanomolar affinity in rat brain, Eur. J. Pharmacol. 192 (1991) 19–24, https://doi.org/10.1016/0014-2999(91)90063-V.